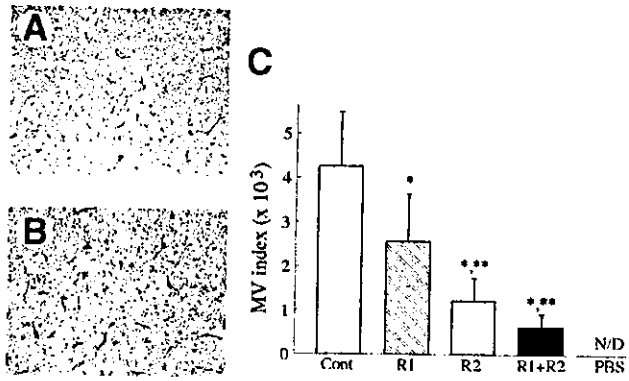

Fig. 7. Immunohistochemical analysis of CD31 expression in HCC. Representative features of the CD31-positive vessels in the tumor at (A) low and (B) high magnification (×40 and ×200, respectively). (C) The semiquantitation of microvessels in the tumor were similar to those of CD31 mRNA expression in the tumor. Of note was the finding that the suppression of angiogenesis by treatment with R1 mAb and R2 mAb was of similar magnitude to that of inhibition of liver neoplasm development. Data represent mean ± SD (n = 5). Cont, control IgG-treated mice (1,000 μg/mouse [G1]); R1 and R2, R1 mAb- and R2 mAb-treated mice (1,000 μg/mouse [G2 and G3, respectively]); R1 + R2, R1 mAb and R2 mAb combination-treated group (G4); phosphate buffer saline-treated group (G5); N/D: not detected. *Statistically significant difference from G1 ($P < .01$). **Statistically significant difference from G2 ($P < .05$). MV, microvessel.

not altered by the administration of R2 mAb and R1 mAb, respectively (Fig. 6).

Lung Metastasis. We observed lung tumors that were clearly discriminated from the surrounding tissues in the DEN-treated groups (Fig. 1C); histological examination revealed that these tumors were metastatic tumors from HCC (Fig. 1D). We analyzed the incidence and counted the metastatic lesions in the lung. Of 10 DEN-treated control mice, 8 showed lung metastasis (Table 2). Treatment with R1 mAb and R2 mAb markedly suppressed the development of lung metastasis (4/10 and 2/10, respectively). No lung metastasis could be found in the group treated with R1 mAb and R2 mAb in combination. Similar to tumor incidence, the number of lesions was significantly suppressed by treatment with R1 mAb and R2 mAb as compared to the control group ($P < .01$), and R2 mAb exerted a stronger inhibition than R1 mAb ($P < .05$).

Discussion

Angiogenesis is a complex and critical process essential to support the growth of solid tumors.[1,2] This concept is supported by a large body of evidence demonstrating that any solid tumor can not grow even beyond a few millimeters in size without angiogenesis. It was considered that angiogenesis initiated the increase in tumor diameter from several hundred microns to 1 mm when the tumor mass contained roughly 10^5 to 10^6 cells.[39] However, it has been recently reported that angiogenesis can also be induced at the early stages of tumor formation and carcinogenic procedures in several types of experimental models, such as the RIP1-Tag2 pancreatic β-cell islet carcinoma in transgenic mice.[4] In this model, treatment with a small-molecule inhibitor of VEGF receptors resulted in a significant reduction in the number of angiogenic islets and in substantial reduction of tumor growth.[40] In agreement with these studies, we found that neovascularization was increased stepwise during hepatocarcinogenesis. We also observed that suppression of the VEGF and receptor interaction by treatment with VEGF receptor mAbs significantly attenuated hepatocarcinogenesis in addition to inhibiting neovascularization. It has been reported that VEGFR-2 plays a more important role both *in vitro* and *in vivo* in several biological events.[19-22] However, recent studies have revealed that VEGFR-1 plays important roles under certain pathological conditions, such as tumor growth.[24-26] The other VEGF homologue—namely, the placental growth factor that binds VEGFR-1 but not VEGFR-2—in the knockout mice inhibited the pathological angiogenesis.[41] The lung carcinoma cells overexpressing placental growth factor grew much faster in the wild-type mice than in the VEGFR-1 tyrosine-kinase domain-deficient knockout mice.[25] In the present study, we found that inhibition of either VEGFR-1 or VEGFR-2 significantly attenuated liver carcinogenesis along with angiogenesis suppression, and that treatment with R2 mAb was more potent than treatment with R1 mAb. The combination treatment with both mAbs almost completely attenuated liver carcinogenesis. These results indicated that, in addition to VEGFR-2, VEGFR-1 also played an important role in the process of hepatocarcinogenesis. Further mechanistic studies to elucidate whether R1 mAb and R2mAb attenuate cell transformation or influence the preneoplastic lesion growth should be performed in the future.

There is also increasing evidence to support the concept that metastasis from solid tumors is facilitated by

Table 2. Effect of R1 mAb and R2 mAb on Lung Metastasis of DEN-Induced HCC

	Incidence	No. of Lesions (per mouse)
Control	8/10	6.4 ± 1.4
R1 mAb	4/10	2.7 ± 0.7*
R2 mAb	2/10	1.0 ± 0.5*†
R1 + R2 mAb	0/10	–
PBS	0/10	–

*$P < .01$ vs. control.
†$P < .05$ vs. R1mAb.

angiogenesis in the primary tumor. Although not all angiogenic tumors produce metastases, inhibition of angiogenesis prevents the growth of tumors as well as metastases.[42] Antisense VEGF gene transfer reportedly inhibited lung metastases from HCC.[43] It has also been reported that tumor VEGF expression level correlates with intrahepatic metastasis in human samples.[44,45] However, to date, there is no report elucidating the role of VEGF in spontaneous organ metastasis from HCC. In the current study, we observed that inhibition of VEGF and receptor interaction significantly attenuated spontaneous lung metastases of HCC. Both VEGFR-1 and VEGFR-2 were involved in the lung metastasis from HCC, and, similar to the carcinogenesis step, signaling through VEGFR-2 was a predominant pathway compared to that of VEGFR-1.

One of the characteristic features of HCC in clinical practice is hypervascularity. In fact, VEGF expression was reportedly upregulated in the HCC tumor tissue compared to adjacent noncancerous lesions.[15–17] Previously, we reported that overexpression of VEGF correlated with a marked increase in HCC development, in addition to augmentation of neovascularization, whereas suppression of VEGF led to a decrease in HCC growth.[18] We have reported that suppression of VEGFR-2 significantly attenuated HCC growth.[23] In addition to VEGFR-2, we have found that R1 mAb treatment also significantly suppresses HCC development in subcutaneous and orthotopic transplantation models.[46] Taken together, the suppression of VEGF and receptor attenuated not only the hepatocarcinogenic process but also HCC growth.

Although several alternative therapies have been employed for HCC, there is still no satisfactory prognostic improvement of HCC. One of the reasons for the poor prognosis in HCC is the high rate of recurrence.[47,48] It has been shown that this high recurrence rate, even after curative therapy, is due to intrahepatic metastasis or multicentric development of each neoplasm clone, and it is known that most cases of HCC are patients with chronic hepatitis and liver cirrhosis. Since the high-risk group for HCC development seems to be clearer than in other types of cancer, it is likely that a primary or secondary chemopreventive agent would be beneficial in improving the prognosis of HCC. It is possible that in the future antibodies targeting VEGF receptors could be used as chemopreventive and suppressive agents against HCC development.

In summary, hepatic VEGF expression and angiogenic response increased stepwise during hepatocarcinogenesis, and both R1 mAb and R2 mAb treatment significantly attenuated HCC development in addition to suppressing neovascularization. The inhibitory effect of R2 mAb was more potent than that of R1 mAb, and combination treatment with R1 mAb and R2 mAb almost completely attenuated hepatocarcinogenesis. Spontaneous lung metastasis from HCC was also significantly suppressed by R1 mAb and R2 mAb. These results suggest that the interaction of VEGF and receptor plays an important role in hepatocarcinogenesis and spontaneous lung metastasis from HCC.

References

1. Carmeliet P, Jain RK. Angiogenesis in cancer and other diseases. Nature 2000;407:249–257.
2. Kerbel RS. Tumor angiogenesis: past, present and the near future. Carcinogenesis 2000;21:505–515.
3. Saaristo A, Karpanen T, Alitalo K. Mechanisms of angiogenesis and their use in the inhibition of tumor growth and metastasis. Oncogene 2000;19: 6122–6129.
4. Bergers G, Javaherian K, Lo KM, Folkman J, Hanahan D. Effects of angiogenesis inhibitors on multistage carcinogenesis in mice. Science 1999;284:808–812.
5. Bolontrade MF, Stern MC, Binder RL, Zenklusen JC, Gimenez-Conti IB, Conti CJ. Angiogenesis is an early event in the development of chemically induced skin tumors. Carcinogenesis 1998;19:2107–2113.
6. Frachon S, Gouysse G, Dumortl J, Couvelard A, Nejjari M, Mion F, et al. Endothelial cell marker expression in dysplastic lesions of the liver: an immunohistochemical study. J Hepatol 2001;34:850–857.
7. Park YN, Kim YB, Yang KM, Park C. Increased expression of vascular endothelial growth factor and angiogenesis in the early stage of multistep hepatocarcinogenesis. Arch Pathol Lab Med 2000;124:1061–1065.
8. Kin M, Torimura T, Ueno T, Nakamura T, Ogata R, Sakamoto M, et al. Angiogenesis inhibitor TNP-470 suppresses the progression of experimentally-induced hepatocellular carcinoma in rats. Int J Oncol 2000;16:375–382.
9. Ferrara N. VEGF: an update on biological and therapeutic aspects. Curr Opin Biotechnol 2000;11:617–624.
10. Shibuya M. Structure and function of VEGF/VEGF-receptor system involved in angiogenesis. Cell Struct Funct 2001;26:25–35.
11. Alon T, Hemo I, Itin A, Pe'er J, Stone J, Keshet E. Vascular endothelial growth factor acts as a survival factor for newly formed retinal vessels and has implications for retinopathy of prematurity. Nat Med 1995;1:1024–1028.
12. Bruns CJ, Liu W, Davis DW, Shaheen RM, McConkey DJ, Wilson MR, et al. Vascular endothelial growth factor is an in vivo survival factor for tumor endothelium in a murine model of colorectal carcinoma liver metastases. Cancer 2000;89:488–499.
13. Yamane A, Seetharam L, Yamaguchi S, Gotoh N, Takahashi T, Neufeld G, et al. A new communication system between hepatocytes and sinusoidal endothelial cells in liver through vascular endothelial growth factor and Flt tyrosine kinase receptor family (Flt-1 and KDR/Flk-1). Oncogene 1994; 9:2683–2690.
14. Inoue M, Hager JH, Ferrara N, Gerber HP, Hanahan D. VEGF-A has a critical, nonredundant role in angiogenic switching and pancreatic beta cell carcinogenesis. Cancer Cell 2002;1:193–202.
15. Yamaguchi R, Yano H, Nakashima Y, Ogasawara S, Higaki K, Akiba J, et al. Expression and localization of vascular endothelial growth factor receptors in human hepatocellular carcinoma and non-HCC tissues. Oncol Rep 2000;7:725–729.
16. Suzuki K, Hayashi N, Miyamoto Y, Yamamoto M, Ohkawa K, Ito Y, et al. Expression of vascular permeability factor/vascular endothelial growth factor in human hepatocellular carcinoma. Cancer Res 1996;56:3004–3009.
17. Mise M, Arii S, Higashituji H, Furutani M, Niwano M, Harada T, et al. Clinical significance of vascular endothelial growth factor and basic fibroblast growth factor gene expression in liver tumor. HEPATOLOGY 1996;23: 455–464.

18. Yoshiji H, Kuriyama S, Yoshii J, Yamazaki M, Kikukawa M, Tsujinoue H, et al. Vascular endothelial growth factor tightly regulates in vivo development of murine hepatocellular carcinoma cells. HEPATOLOGY 1998;28: 1489-1496.
19. Waltenberger J, Claesson-Welsh L, Siegbahn A, Shibuya M, Heldin CH. Different signal transduction properties of KDR and Flt1, two receptors for vascular endothelial growth factor. J Biol Chem 1994;269:26988–26995.
20. Millauer B, Wizigmann-Voos S, Schnurch H, Martinez R, Moller NP, Risau W, et al. High affinity VEGF binding and developmental expression suggest Flk-1 as a major regulator of vasculogenesis and angiogenesis. Cell 1993;72:835–846.
21. Millauer B, Longhi MP, Plate KH, Shawver LK, Risau W, Ullrich A, et al. Dominant-negative inhibition of Flk-1 suppresses the growth of many tumor types in vivo. Cancer Res 1996;56:1615–1620.
22. Skobe M, Rockwell P, Goldstein N, Vosseler S, Fusenig NE. Halting angiogenesis suppresses carcinoma cell invasion. Nat Med 1997;3:1222–1227.
23. Yoshiji H, Kuriyama S, Hicklin DJ, Huber J, Yoshii J, Miyamoto Y, et al. KDR/Flk-1 is a major regulator of vascular endothelial growth factor-induced tumor development and angiogenesis in murine hepatocellular carcinoma cells. HEPATOLOGY 1999;30:1179–1186.
24. Shibuya M. Structure and dual function of vascular endothelial growth factor receptor-1 (Flt-1). Int J Biochem Cell Biol 2001;33:409–420.
25. Hiratsuka S, Maru Y, Okada A, Seiki M, Noda T, Shibuya M. Involvement of Flt-1 tyrosine kinase (vascular endothelial growth factor receptor-1) in pathological angiogenesis. Cancer Res 2001;61:1207–1213.
26. Hiratsuka S, Nakamura K, Iwai S, Murakami M, Itoh T, Kijima H, et al. MMP9 induction by vascular endothelial growth factor receptor-1 is involved in lung-specific metastasis. Cancer Cell 2002;2:289–300.
27. Lyden D, Hattori K, Dias S, Costa C, Blaikie P, Butros L, et al. Impaired recruitment of bone-marrow-derived endothelial and hematopoietic precursor cells blocks tumor angiogenesis and growth. Nat Med 2001;7:1194–1201.
28. Luttun A, Tjwa M, Moons L, Wu Y, Angelillo-Scherrer A, Liao F, et al. Revascularization of ischemic tissues by PlGF treatment, and inhibition of tumor angiogenesis, arthritis and atherosclerosis by anti-Flt1. Nat Med 2002;8:831–840.
29. Prewett M, Huber J, Li Y, Santiago A, O'Connor W, King K, et al. Antivascular endothelial growth factor receptor (fetal liver kinase 1) monoclonal antibody inhibits tumor angiogenesis and growth of several mouse and human tumors. Cancer Res 1999;59:5209–5218.
30. Yoshiji H, Nakae D, Kinugasa T, Matsuzaki M, Denda A, Tsujii T, et al. Inhibitory effect of dietary iron deficiency on the induction of putative preneoplastic foci in rat liver initiated with diethylnitrosamine and promoted by phenobarbital. Br J Cancer 1991;64:839–842.
31. Shiota G, Harada K, Ishida M, Tomie Y, Okubo M, Katayama S, et al. Inhibition of hepatocellular carcinoma by glycyrrhizin in diethylnitrosamine-treated mice. Carcinogenesis 1999;20:59–63.
32. Yoshiji H, Kuriyama S, Hicklin DJ, Huber J, Yoshii J, Ikenaka Y, et al. The vascular endothelial growth factor receptor KDR/Flk-1 is a major regulator of malignant ascites formation in the mouse hepatocellular carcinoma model. HEPATOLOGY 2001;33:841–847.
33. Yoshiji H, Kuriyama S, Yoshii J, Ikenaka Y, Noguchi R, Hicklin DJ, et al. Synergistic effect of basic fibroblast growth factor and vascular endothelial growth factor in murine hepatocellular carcinoma. HEPATOLOGY 2002;35: 834–842.
34. Moser GJ, Wong BA, Wolf DC, Fransson-Steen RL, Goldsworthy TL. Methyl tertiary butyl ether lacks tumor-promoting activity in N-nitrosodiethylamine-initiated B6C3F1 female mouse liver. Carcinogenesis 1996; 17:2753–2761.
35. Ward JM. Morphology of hepatocellular neoplasmas in B6C3F1 mice. Cancer Lett 1980;9:319–325.
36. Yoshiji H, Kuriyama S, Yoshii J, Ikenaka Y, Noguchi R, Nakatani T, et al. Angiotensin-II type 1 receptor interaction is a major regulator for liver fibrosis development in rats. HEPATOLOGY 2001;34:745–750.
37. Yoshiji H, Harris SR, Thorgeirsson UP. Vascular endothelial growth factor is essential for initial but not continued in vivo growth of human breast carcinoma cells. Cancer Res 1997;57:3924–3928.
38. Takahashi T, Shibuya M. The 230 kDa mature form of KDR/Flk-1 (VEGF receptor-2) activates the PLC-gamma pathway and partially induces mitotic signals in NIH3T3 fibroblasts. Oncogene 1997;14:2079–2089.
39. Folkman J. Tumor angiogenesis: therapeutic implications. N Engl J Med 1971;285:1182–1186.
40. Bergers G, Brekken R, McMahon G, Vu TH, Itoh T, Tamaki K, et al. Matrix metalloproteinase-9 triggers the angiogenic switch during carcinogenesis. Nat Cell Biol 2000;2:737–744.
41. Carmeliet P, Moons L, Luttun A, Vincenti V, Compernolle V, De Mol M, et al. Synergism between vascular endothelial growth factor and placental growth factor contributes to angiogenesis and plasma extravasation in pathological conditions. Nat Med 2001;7:575–583.
42. Fidler IJ, Ellis LM. The implications of angiogenesis for the biology and therapy of cancer metastasis [comment]. Cell 1994;79:185–188.
43. Tang Z, Zhou X, Lin Z, Yang B, Ma Z, Ye S, et al. Surgical treatment of hepatocellular carcinoma and related basic research with special reference to recurrence and metastasis. Chin Med J (Engl) 1999;112:887–891.
44. Poon RT, Ng IO, Lau C, Zhu LX, Yu WC, Lo CM, et al. Serum vascular endothelial growth factor predicts venous invasion in hepatocellular carcinoma: a prospective study. Ann Surg 2001;233:227–235.
45. Ng IO, Poon RT, Lee JM, Fan ST, Ng M, Tso WK. Microvessel density, vascular endothelial growth factor and its receptors Flt-1 and Flk-1/KDR in hepatocellular carcinoma. Am J Clin Pathol 2001;116:838–845.
46. Yoshiji H, Kuriyama S, Yoshii J, Ikenaka Y, Noguchi R, Yanase K, et al. Involvement of the vascular endothelial growth factor receptor-1 (VEGFR-1) in murine hepatocellular carcinoma development. J Hepatol 2004. In press.
47. Schafer DF, Sorrell MF. Hepatocellular carcinoma. Lancet 1999;353:1253–1257.
48. Befeler AS, Di Bisceglie AM. Hepatocellular carcinoma: diagnosis and treatment. Gastroenterology 2002;122:1609–1619.

ELSEVIER

Journal of Hepatology 41 (2004) 97–103

Journal of Hepatology

www.elsevier.com/locate/jhep

Involvement of the vascular endothelial growth factor receptor-1 in murine hepatocellular carcinoma development

Hitoshi Yoshiji[1,*], Shigeki Kuriyama[2], Junichi Yoshii[1], Yasuhide Ikenaka[1], Ryuichi Noguchi[1], Koji Yanase[1], Tadashi Namisaki[1], Mitsuteru Kitade[1], Masaharu Yamazaki[1], Hirohisa Tsujinoue[1], Tsutomu Masaki[2], Hiroshi Fukui[1]

[1]*Third Department of Internal Medicine, Nara Medical University, Shijo-cho 840, Kashihara, 634-8522 Nara, Japan*
[2]*Third Department of Internal Medicine, School of Medicine, Kagawa University, Kagawa, Japan*

***Background/Aims*: The role of the vascular endothelial growth factor receptor-1 (VEGFR-1) in hepatocellular carcinoma (HCC) development has not been elucidated yet. The aim of this study was to examine the role of VEGFR-1 in VEGF-mediated HCC development and angiogenesis as compared to that of VEGFR-2.**

***Methods*: We examined the effects of VEGFR-1, and VEGFR-2 neutralizing monoclonal antibodies (R-1mAb and R-2mAb, respectively) on VEGF-mediated HCC development both in an allograft and orthotopic models.**

***Results*: In the allograft model, both R-1mAb and R-2mAb significantly attenuated the VEGF-mediated tumor development in a dose dependent manner with associated reduction of angiogenesis in the tumor. The inhibitory effect of R-2mAb was more potent than that of R-1mAb, and the combination treatment with both mAbs almost completely attenuated VEGF-mediated HCC development. Immunohistochemical analysis revealed that apoptosis increased markedly in the tumor. Furthermore, these inhibitory effects with both mAbs were achieved even on established tumors and orthotopic transplantation.**

***Conclusions*: In addition to VEGFR-2, VEGFR-1 also lies on the signal transduction pathway by which VEGF augments HCC development and angiogenesis not only at the initial stage but also in the established tumor.**

Keywords: **VEGF; flt-1 (VEGFR-1); KDR/Flk-1 (VEGFR-2); Hepatocellular carcinoma; Angiogenesis**

1. Introduction

The growth of any solid tumor, including hepatocellular carcinoma (HCC) is now widely recognized to depend on the process of neovascularization [1–3]. Among the identified pro-angiogenic factors, the vascular endothelial growth factor (VEGF) is the most intriguing factor with regard to the angiogenesis process [4,5]. In the human specimens, the increased expression of VEGF correlated with aggressive behavior and poor prognosis. In the animal experimental models, overexpression of VEGF enhanced tumor growth, whereas suppression of VEGF inhibited tumor growth [4–6]. Two tyrosine kinases, *fms*-like tyrosine kinase (flt-1: VEGFR-1) and the kinase insert domain-containing receptor/murine homologue, fetal liver kinase-1 (KDR/Flk-1: VEGFR-2), both of which are type III tyrosine kinase receptors, have been identified as the main VEGF receptors. Although VEGFR-1 shows affinity to VEGF at least 10-fold higher than VEGFR-2, it has been reported that VEGFR-2 is a major positive signal transducer through its strong tyrosine kinase activity as compared to VEGFR-1 both in vitro and in vivo [4,5,7–10]. However, recent studies have revealed that VEGFR-1 has a dual function in angiogenesis, acting in a positive or negative manner under different conditions [11]. In physiological angiogenesis, such as embryo development, VEGFR-1 exerts a negative regulatory function, probably via its strong VEGF-trapping activity [12]. It has been revealed that VEGFR-1 can act as a potent positive regulator of VEGF under pathological conditions, such as tumor angiogenesis [13]. Furthermore, it has been reported that VEGFR-1 is an important mediator in tumor angiogenesis,

Received 9 December 2003; received in revised form 13 February 2004; accepted 12 March 2004; available online 12 April 2004
* Corresponding author. Tel.: +81-744-22-3051; fax: +81-744-24-7122.
E-mail address: yoshijih@naramed-u.ac.jp (H. Yoshiji).

0168-8278/$30.00
doi:10.1016/j.jhep.2004.03.001

arthritis, and arteriosclerosis via bone marrow-derived hematopoietic stem-cell recruitment, and mobilization [14].

HCC is one of the most prevalent malignancies worldwide and causes more than one million deaths annually, and its incidence continues to increase not only in Asia but also in the United States [15,16]. One of the representative characteristic features of HCC in the clinical practice is hypervascularity. Several studies showed that angiogenesis was implicated in survival and growth of HCC. It has been reported that VEGF expression was up-regulated in the tumors of HCC as compared to the non-cancerous lesions, and that overexpression of VEGF exerted a marked increase in HCC development accompanied by augmentation of neovascularization [17–21]. We have reported that inhibition of VEGFR-2 with the neutralizing monoclonal antibody (R-2mAb) significantly suppressed the HCC development associated with suppression of angiogenesis [22]. However, it is still unknown whether VEGFR-1 plays some biological roles and coordinates with VEGFR-2 in HCC development and angiogenesis.

The tetracycline-controlled transactivator-responsive promoter (Tet-system) is a novel drug-regulated gene expressing system, because it can manipulate the gene of interest in an 'on and off' manner in vivo [23]. We used a modified retrovirus-mediated vector (Retro-Tet) system to achieve tighter regulation and less leaky background basal expression than the original Tet system as described previously [21,24–26]. With this modified Retro-Tet system, it is possible to observe the tumor kinetics that can be achieved by VEGF gene expression.

In our present study, we examined the roles of VEGFR-1 and VEGFR-2 in HCC development and angiogenesis at different stages by means of combination of the Retro-Tet system, specific neutralizing monoclonal antibodies of VEGFR-1, and VEGFR-2 (R-1mAb and R-2mAb, respectively). Furthermore, since the orthotopic transplantation has been reported to show a preferential site of growth of the transplanted tumor cells [27,28], we also examined the inhibitory effects of R-1mAb and R-2mAb on the development of HCC in the liver.

2. Methods

2.1. Construction of the vector, cell culture, and compounds

A complete description of the construction of the Retro-Tet vector, in which the human VEGF cDNA was inserted (Tet-VEGF), and stable Tet-VEGF-expressing BNL.1ME A 7R. 1 HCC (Tet-VEGF-HCC) has been reported previously [21]. This BNL-HCC cell line expressed neither VEGFR-1 nor VEGFR-2 as described previously [21,22]. The cells were grown in media recommended by the suppliers. The R-1mAb and R-2mAb were generated as described previously [22,29–31], and the specific neutralization of their respective receptors were reported elsewhere [14,32].

2.2. Animal treatment

In an allograft model, 1×10^6 Tet-VEGF-cells or *lacZ*-HCC cells were syngenetically inoculated into the flank of BALB/c mice. At first, we performed a dose-dependent study. Either R-1mAb or R-2mAb was intraperitoneally (i.p.) injected twice a week at doses of 400 and 800 μg/mouse, respectively. As a negative control, the same amount of immunoglobulin G (IgG) was injected as described previously [22,31]. To examine the combination effect of both mAbs, 800 μg/mouse of R-1mAb and R-2mAb were administered simultaneously. The next experiment was conducted to examine the effects of mAbs on the fully established tumor growth. In this experiment, either R-1mAb or R-2mAb administration was started on day 24 (the mean tumor volume was 827 mm^3). To suppress the VEGF expression in the Tet-VEGF tumor, the mice were given Tet-containing water (1 mg/ml) through the experiment. The tumor volume was measured twice a week, and the mice were killed 48 days after the tumor cell implantation under anesthesia. In the allograft studies, each experimental group consisted of eight mice. For the direct liver injection experiment, 1×10^6 of Tet-VEGF or *LacZ*- transduced BNL-HCC cells were directly injected into the liver ($n = 7$ for each group). The cells were suspended in 10 μl of PBS and implanted directly under the capsule of the left-lateral hepatic lobe under direct visualization, by means of a 10-μl Hamilton syringe with a 26-gauge needle over a period of 2–3 min. Treatments with R-1mAb and R-2mAb were the same as in the xenograft experiments. Fourteen days after the injection, the mice were killed and examined macro and microscopically for HCC development in the liver. All animal procedures were performed according to approved protocols and in accordance with the standard recommendations for the proper care and use of laboratory animals.

2.3. Immunohistochemical examination

For determination of the in vivo angiogenesis, we employed immunohistochemical detection of CD31 in frozen sections of tumors having the same size to avoid the necrotic effect of hypoxia with a primary rat anti-mouse CD31 antibody (Pharmingen, San-Diego, CA, USA) as described previously [22,26,33]. These immunopositive vessels were evaluated with Adobe Photoshop and NIH image software as described previously [22,26,33]. Apoptosis was detected with the DNA fragmentation products that were stained by in situ 3′ end labeling (terminal deoxynucleotidyl transferase-mediated dUTP nick labeling) [TUNEL] with paraffin-embedded sections as described previously [31,34,35]. For each tumor, the positive cells in 30 high-power fields at a magnification of × 400 were examined.

2.4. Immunoprecipitation and Western blotting

To examine the effect of R-1mAb and R-2mAb on autophosphorylation and protein expression of the respective receptors in the tumor, immunoprecipitation (IP) and Western blotting (WB) were performed as previously described [22,31]. The tumor pool lysate solution was concentrated and used for IP and WB. To conduct IP, the tumor lysates were immunoprecipitated with anti-phosphotyrosine before conducting SDS-PAGE. Anti-tyrosine (4G10) was purchased from Upstate Biotechnology (NY, USA) and anti-VEGFR-2 (C-1158), VEGFR-1 (C-17) were obtained from Santa-Cruz (CA, USA).

2.5. Statistical analysis

To assess the statistical significance of the inter-group differences in the quantitative data, the Mann–Whitney *U* test was used to compare the mean values between two groups. The Kruskal–Wallis test was used to compare the mean values between more than two groups.

3. Results

3.1. Tumor growth kinetics in VEGF-mediated HCC development

When VEGF expression in the tumor was up-regulated with Tet-free normal water, the tumor growth rate was significantly augmented as compared with the *lacZ*-transduced

control group. On the contrary, when the VEGF expression was shut down by administering Tet-containing water (1 mg/ml) to the mice, the tumor growth was significantly decreased to almost the same level as the control (Fig. 1). These results indicated that the increased tumor growth kinetics in this study were exclusively due to VEGF overexpression.

To examine the roles of VEGFR-1 and VEGFR-2 in VEGF-induced HCC tumor development, the respective mAb was injected i.p. into mice bearing Tet-VEGF–HCC cells. At first, we examined the effect of R-1 mAb on the primary tumor growth in the allograft model. As shown in Fig. 1, the tumor development in the R-1mAb-treated groups at doses of 400 and 800 μg/mouse was significantly suppressed as compared to the IgG-treated group ($P < 0.05$ and $P < 0.01$, respectively). The treatment at 800 μg/mouse exerted a further inhibitory effect as compared with that at a dose of 400 μg/mouse ($P < 0.05$). We next performed the same experiment with R-2mAb. In accordance with a previous report [22], R-2mAb treatment significantly attenuated the VEGF-mediated HCC development. Similar to R-1mAb, R-2mAb treatment at a dose of 800 μg/mouse showed a more potent inhibitory effect than at 400 μg/ mouse in a dose ranging study ($P < 0.05$) (Fig. 2). At a dose of 800 μg/mouse, the inhibitory impact was more potent with R-2mAb than that of R-1mAb ($P < 0.05$). The combination treatment with both mAbs revealed further inhibition as compared with that of R-2mAb alone ($P < 0.05$). This combination treatment almost completely attenuated the VEGF-induced HCC development (Fig. 3).

We also examined whether the inhibitory effects of these mAbs could be found even after the tumor was established.

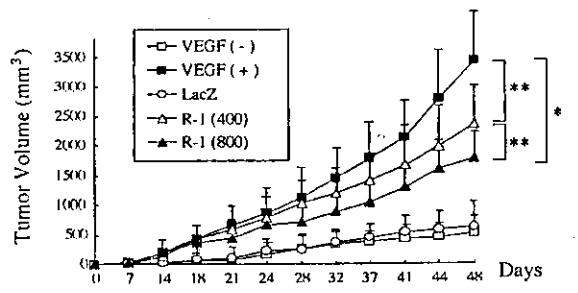

Fig. 1. The effect of R-1mAb-mediated suppression on the VEGF-induced HCC development. To maintain VEGF overexpression or suppression, the mice were given Tet-free normal and Tet-containing drinking water, respectively. The *lacZ* HCC-injected mice served as a negative control. These groups were injected with control IgG. The R-1mAb was i.p. administered twice a week. The R-1mAb treatment significantly attenuated the VEGF-mediated HCC development in a dose dependent manner. The tumor volume was determined by three-dimensional calipers at the indicated time points. Each point represents the mean ± SD ($n = 8$). *, **: Statistically significant differences between the indicated groups ($P < 0.01$ and $P < 0.05$, respectively). VEGF (+) and VEGF (−): VEGF overexpression and suppression in the tumor, respectively. R-1 (400) and R-1 (800): The mice with VEGF over-expressing tumor were treated with R-1mAb at doses of 400 and 800 μg/mouse, respectively.

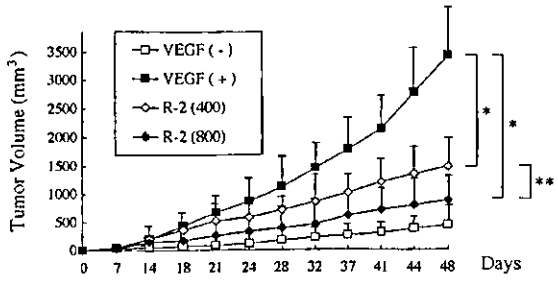

Fig. 2. The effect of R-2mAb-mediated suppression on the VEGF-induced HCC development. The R-2mAb was i.p. administered twice a week from the beginning of the experiment. The R-2mAb treatment also significantly attenuated the VEGF-mediated HCC development in a dose dependent manner. The tumor volume was determined by three-dimensional calipers at the indicated time points. Each point represents the mean ± SD ($n = 8$). *, **: Statistically significant differences between the indicated groups ($P < 0.01$ and $P < 0.05$, respectively). VEGF (+) and VEGF (−): VEGF overexpression and suppression in the tumor, respectively. R-2 (400) and R-2 (800): the mice with VEGF over-expressing tumor were treated with R-2mAb at doses of 400 and 800 μg/mouse, respectively.

When the mean tumor volume reached about 845 mm^3, either R-1mAb or R-2mAb treatment at a dose of 800 μg/mouse was started twice a week. As shown in Fig. 4, the R-1mAb and R-2mAb treatments exerted significant inhibitory effects as compared with the control group even after the tumor was fully established ($P < 0.05$ and $P < 0.01$, respectively). Noteworthy is the fact that the combination treatment with R-1mAb and R-2mAb almost achieved a dormancy status of the established tumor.

We next examined the effects of R-1mAb and R-2mAb on HCC development in the liver direct injection experiment. Similar to the results of allograft studies, both R-1mAb and R-2 mAb significantly suppressed the number and size of HCC development in the liver (Table 1). Neither tumor invasion into other organs nor metastasis was

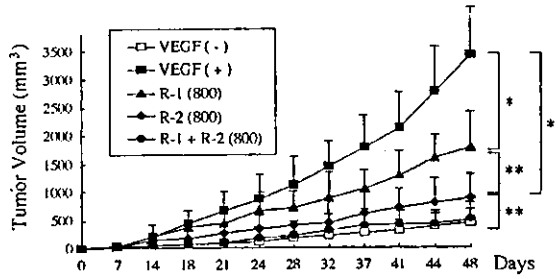

Fig. 3. The effect of combination treatment of R-1mAb and R-2mAb on the VEGF-induced HCC development. R-1mAb and R-2mAb were i.p. administered twice a week from the beginning of the experiment. The R-1mAb and R-2mAb combination treatment almost completely attenuated the VEGF-induced HCC development. The tumor volume was determined by three-dimensional calipers at the indicated time points. R-1 (800), R-2 (800): R-1mAb and R-2mAb-treated group at a dose of 800 μg/mouse, respectively. R-1 + R-2 (800): R-1mAb and R-2mAb combination-treated group at a dose of 800 μg/mouse. Each point represents the mean ± SD ($n = 8$). *, **: Statistically significant differences between the indicated groups ($P < 0.01$ and $P < 0.05$, respectively).

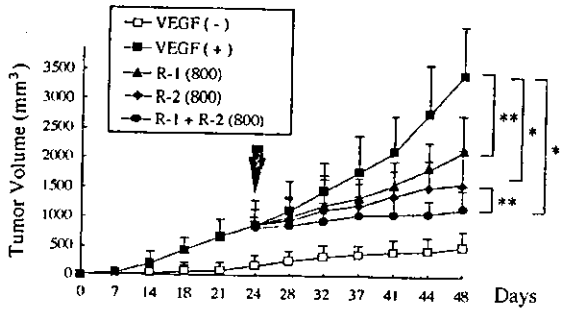

Fig. 4. The inhibitory effects of R-1mAb and R-2mAb against established tumors. The mice received either R-1mAb or R-2mAb at a dose of 800 μg/ml from day 24 (the mean tumor volume was 845 mm³). The R-1mAb and R-2mAb treatments exerted significant inhibitory effects as compared with the control group even after the tumor was established. The arrows indicate the time points of administration of the respective mAb. Each point represents the mean ± SD (each group consisted of eight mice). *, **: Statistically significant differences between the indicated groups ($P < 0.01$ and $P < 0.05$, respectively).

observed at the sacrifice time both in the allograft and orthotopic studies, and the systemic administration of neither R-1mAb nor R-2mAb had any apparent effect on the state of health of the mice (data not shown).

3.2. Tumor neovascularization

To determine whether the inhibitory effects of R-1mAb and R-2mAb on the tumor development were accompanied by suppression of neovascularization, we examined the expression level of CD31 in the tumor. As shown in Fig. 5, similar to the result of HCC development, the CD31-positive vessels in the tumors of either R-1mAb or R-2mAb-treated groups (800 μg/mouse) were significantly fewer

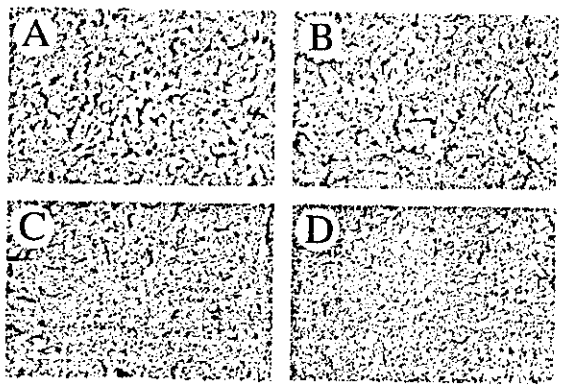

Fig. 5. The effects of R-1mAb and R-2mAb on CD31 expression in the tumors. The tumor vascularization was visualized by immunostaining of the CD31 vascular endothelial adhesion protein. (A) Tet-VEGF-HCC control group; (B) R-1mAb-treated group; (C) R-2mAb-treated group; (D) R-1mAb and R-2mAb combination-treated group. The description of each group is shown in Section 2. Original magnification was × 200.

Table 1
Effect of R-1 mAb and R-2 mAb on HCC development in the liver

	Number of tumors in the liver/mouse				Incidence of large tumor in the liver[a]
VEGF	29 ± 9[b]	**	*	*	7/7 (100%)
R-1 mAb	20 ± 6	*			7/5 (71%)
R-2 mAb	7 ± 4	*			7/2 (29%)
R-1 + R-2 mAbs	2 ± 1				7/0 (0%)

*$P < 0.01$ and **$P < 0.05$ between the indicated groups.
[a] A large tumor is over 5 mm in diameter.
[b] Data are expressed as mean ± SD ($n = 7$).

than those in the control (IgG-treated) group. The combination treatment with R-1mAb and R-2mAb almost attenuated the CD31-positive vessels in the tumor. A semi-quantitative analysis of the CD31-positive vessels in R-1mAb or R-2mAb revealed a statistically significant suppression as compared to the control group ($P < 0.01$). Similar to the tumor growth suppression, the inhibitory effect of R-2mAb was more potent than that of R-1mAb ($P < 0.05$). The combination treatment with R-1mAb and R-2mAb exerted a much stronger inhibition of the CD31-positive vessels in the tumor as compared to the treatment with R-2mAb alone ($P < 0.05$) (Fig. 6A). Neither R-1mAb nor R-2mAb altered the vascularization in the other normal organs, such as the lung and heart (data not shown).

3.3. Effect of R-1mAb and R-2mAb on apoptosis in vivo

We next examined whether the tumor inhibition by R-1mAb and R-2mAb was reflected by apoptosis in the tumor. As shown in Fig. 6B, the TUNEL-positive apoptotic cells more markedly increased with R-1mAb or R-2mAb treatment (800 μg/mouse) than in the control group ($P < 0.01$). The number of apoptotic cells with R-2mAb treatment significantly increased as compared to that with R-1mAb treatment ($P < 0.05$), and the combination treatment with R-1mAb and R-2mAb revealed much more TUNEL-positive cells in the tumor than with R-2mAb treatment alone ($P < 0.05$). The incidence of apoptosis in the tumor almost corresponded to the effect of tumor development inhibition. On the contrary, the PCNA-positive cells in the tumor did not show any difference between these mAbs-treated groups and the control group (data not shown).

3.4. Receptors activation in situ

To confirm that R-1mAb and R-2mAb at a dose of 800 μg/mouse actually inhibited autophosphorylation in the tumor, we investigated tyrosine-phosphorylated VEGFR-1 and VEGFR-2 in the tumor after i.p. injection of R-1mAb and R-2mAb. As shown in Fig. 7, the R-1mAb and R-2mAb significantly inhibited tyrosine-phosphorylation of the

respective receptors, and the combination treatment with R-1mAb and R-2mAb almost completely abolished the phosphorylation of both receptors in the tumor. We found co-expression of several bands of phosphorylated VEGFR in the tumor. These bands may reflect the process of additional glycosylations of VEGFR as reported previously [36]. Neither the activation of VEGFR-1 nor that of VEGFR-2 was altered by the administration of R-2mAb and R-1mAb, respectively. The R-1mAb and R-2mAb did not affect the protein expression of their respective receptors, either.

4. Discussion

Using the combination of Retro-Tet system, and specific neutralizing monoclonal antibodies against VEGFR-1 and VEGFR-2, we assessed the role of VEGF and receptor interaction in HCC development. Our data indicate that VEGF and receptor interaction plays a pivotal role in HCC development in a dose dependent manner in not only the initial stage but also when the tumor is fully established in association with angiogenesis suppression. Treatment with either R-1mAb or R-2mAb significantly suppressed the VEGF-induced HCC development, but neither single mAb treatment completely inhibited the tumor development. It has been reported that targeting of either VEGFR-1 or VEGFR-2 alone only partially blocks the growth of Lewis lung cell carcinoma (LLC) tumor, and inhibition of both VEGFR-1 and VEGFR-2 was necessary to completely ablate tumor growth [29]. We also observed that the combination treatment with both mAbs was required to achieve a complete attenuation of HCC tumor development and angiogenesis. These results suggested that, in addition to VEGFR-2, VEGFR-1 exerted a positive role in HCC development and angiogenesis. On the other hand, another report has shown that the LLC cells overexpressing VEGF showed no clear difference in the tumor growth rate between the wild type mice and the VEGFR-1 tyrosine kinase domain-deficient mice [13]. It has recently been reported that recruitment of the bone marrow-derived hematopoietic cells exerts some roles in tumor angiogenesis, and that VEGFR-1 plays an important role in the process [29]. It would be possible that recruitment of bone marrow-derived hematopoietic cells by VEGFR-1 was involved in HCC development in the current study, whereas it was not in the VEGFR-1 tyrosine kinase domain-deficient mice or in the LLC cells.

It is very important to examine whether the tumor shows re-growth or not in long-term study in spite of the continuous treatment with R-1mAb and R-2mAb. Since we killed all animals at the end of experiment (day 48), we unfortunately do not have an exact answer in the current study. However, it has been reported that no relapse of the

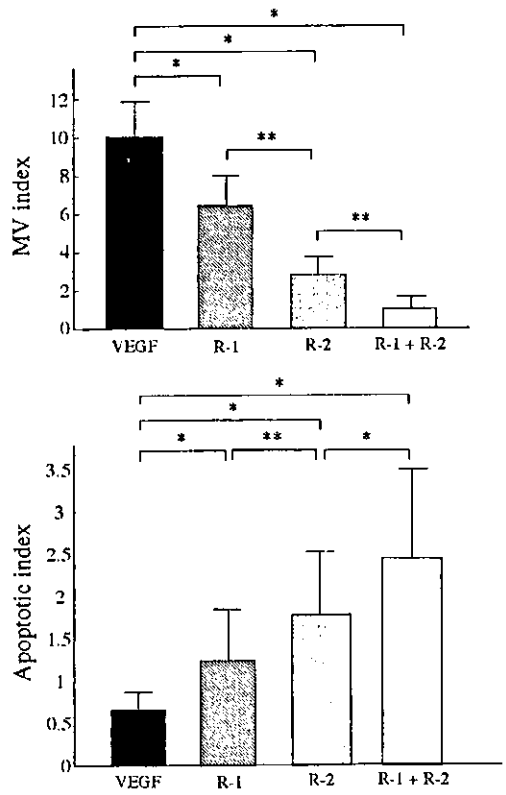

Fig. 6. Semiquantitative analysis of the CD31-immunopositive vessels (A), and the apoptosis (B) in the tumor. The description of each group is shown in Section 2. A semi-quantitative analysis of the CD31-positive vessels in R-1mAb or R-2mAb revealed a statistically significant suppression as compared to the control group. The inhibitory effect of R-2mAb was more potent than that of R-1mAb, and the combination treatment with R-1mAb and R-2mAb exerted a much stronger inhibition of the CD31-positive vessels in the tumor as compared to the treatment with R-2mAb alone. On the contrary, the incidence of apoptosis in the tumor almost corresponded to the effect of tumor development inhibition. R-1, R-2: R-1mAb and R-2mAb-treated group, respectively. R-1 + R-2: R-1mAb and R-2mAb combination-treated group. The data represent the mean ± SD ($n = 5$). *, **: Statistically significant differences between the indicated groups ($P < 0.01$ and $P < 0.05$, respectively). MV: microvessel.

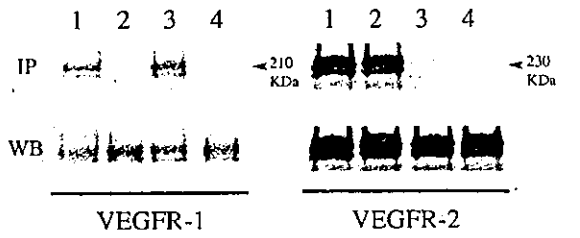

Fig. 7. The effects of R-1mAb and R-2mAb on the activation and protein expression of VEGFR-1 and VEGFR-2 receptors. The R-1mAb and R-2mAb significantly inhibited tyrosine-phosphorylation of the respective receptors. Neither the activation of VEGFR-1 nor that of VEGFR-2 was altered by the administration of R-2mAb and R-1mAb, respectively. The R-1mAb and R-2mAb did not also affect the protein expression of the respective receptors. IP, immunoprecipitation; WB, Western blotting. Lane 1: IgG-treated control group; lane 2: R-1mAb-treated group; lane 3: R-2mAb-treated group; lane 4: R-1mAb and R-2mAb combination-treated group.

tumor was observed with continued administration of R-2mAb at a dose of 400 μg/mouse for up to 120 days in LLC tumor-xenograft model. In addition, withdrawal of R-2mAb treatment resulted in re-growth of the tumors with kinetics similar to those of the control group [32]. Since we used the same antibody at higher dose in the current study, we assume that a similar phenomenon could be observed.

It has been shown that treatment with antiangiogenic agents induces a marked increase of apoptosis in the tumors, whereas it does not alter the tumor cell proliferation [37]. In this study, we noticed similar findings with R-1mAb and R-2mAb. It was an important point to determine whether apoptosis was observed mainly in the endothelial cells (EC) or in the HCC cells. We do not have an exact answer at this time. Although we performed a double immunohistochemical analysis with CD31 and TUNEL in a couple of times, we failed to obtain a good result. The background was very intense, and the interpretation was very difficult (data not shown). It has been suggested that apoptosis of EC occurred first, which led to secondary apoptosis of the tumor cells with antiangiogenic agents [38,39]. We previously found that VEGF did not affect the in vitro proliferation of the BNL-HCC cells, and neither VEGFR-1 nor VEGFR-2 expressed on the HCC cells [21,22]. It has been also reported that VEGFR-1 and VEGFR-2 up-regulated on EC during the tumor angiogenesis, and that VEGF was a survival factor for the tumor EC [4,11,40]. These findings, taken together, suggest that R-1mAb and R-2mAb also first induced the EC apoptosis, and this might induce the secondary apoptosis of the tumor cells. We also found that the R-1mAb and R-2mAb-treated tumors exhibited extensive necrosis accompanied with poor vascularization and increased tumor-cell apoptosis as compared with the large, vascularized control tumors. It has been reported that EC detachment and hemorrhage foci were detected as early as 24 h from VEGF withdrawal in the tumor. In addition at later points, extensive areas of the tumor underwent necrosis [41]. Similar observations were also reported with the R-1mAb-treated human epidermoid tumor in the nude mice [14]. Further studies are required to elucidate the exact mechanism in the future.

In summary, we found that both R-1mAb and R-2mAb significantly attenuated the HCC development in a dose dependent manner along with reduction of angiogenesis in the tumor. The inhibitory effect of R-2mAb was more potent than that of R-1mAb, and the combination treatment with both mAbs almost completely attenuated the VEGF-induced HCC development. Furthermore, these inhibitory effects with both mAbs could be achieved even on the established tumors, and in orthotopic transplantation. These results suggest that, in addition to VEGFR-2, VEGFR-1 also lies on the signal transduction pathway by which VEGF augments HCC development and angiogenesis not only at the initial stage but also after the tumor is fully established.

References

[1] Carmeliet P. Angiogenesis in health and disease. Nat Med 2003;9: 653–660.

[2] Kerbel RS. Tumor angiogenesis: past, present and the near future. Carcinogenesis 2000;21:505–515.

[3] Carmeliet P, Jain RK. Angiogenesis in cancer and other diseases. Nature 2000;407:249–257.

[4] Ferrara N, Gerber HP, LeCouter J. The biology of VEGF and its receptors. Nat Med 2003;9:669–676.

[5] Shibuya M. Structure and function of VEGF/VEGF-receptor system involved in angiogenesis. Cell Struct Funct 2001;26:25–35.

[6] Karkkainen MJ, Petrova TV. Vascular endothelial growth factor receptors in the regulation of angiogenesis and lymphangiogenesis. Oncogene 2000;19:5598–5605.

[7] Kanno S, Oda N, Abe M, Terai Y, Ito M, Shitara K, et al. Roles of two VEGF receptors, Flt-1 and KDR, in the signal transduction of VEGF effects in human vascular endothelial cells. Oncogene 2000;19: 2138–2146.

[8] Kroll J, Waltenberger J. The vascular endothelial growth factor receptor KDR activates multiple signal transduction pathways in porcine aortic endothelial cells. J Biol Chem 1997;272:32521–32527.

[9] Petrova TV, Makinen T, Alitalo K. Signaling via vascular endothelial growth factor receptors. Exp Cell Res 1999;253:117–130.

[10] Waltenberger J, Claesson-Welsh L, Siegbahn A, Shibuya M, Heldin CH. Different signal transduction properties of KDR and Flt1, two receptors for vascular endothelial growth factor. J Biol Chem 1994; 269:26988–26995.

[11] Shibuya M. Structure and dual function of vascular endothelial growth factor receptor-1 (Flt-1). Int J Biochem Cell Biol 2001;33:409–420.

[12] Hiratsuka S, Minowa O, Kuno J, Noda T, Shibuya M. Flt-1 lacking the tyrosine kinase domain is sufficient for normal development and angiogenesis in mice. Proc Natl Acad Sci USA 1998;95:9349–9354.

[13] Hiratsuka S, Maru Y, Okada A, Seiki M, Noda T, Shibuya M. Involvement of Flt-1 tyrosine kinase (vascular endothelial growth factor receptor-1) in pathological angiogenesis. Cancer Res 2001;61: 1207–1213.

[14] Luttun A, Tjwa M, Moons L, Wu Y, Angelillo-Scherrer A, Liao F, et al. Revascularization of ischemic tissues by PlGF treatment, and inhibition of tumor angiogenesis, arthritis and atherosclerosis by anti-Flt1. Nat Med 2002;8:831–840.

[15] Befeler AS, Di Bisceglie AM. Hepatocellular carcinoma: diagnosis and treatment. Gastroenterology 2002;122:1609–1619.

[16] Schafer DF, Sorrell MF. Hepatocellular carcinoma. Lancet 1999;353: 1253–1257.

[17] Mise M, Arii S, Higashituji H, Furutani M, Niwano M, Harada T, et al. Clinical significance of vascular endothelial growth factor and basic fibroblast growth factor gene expression in liver tumor. Hepatology 1996;23:455–464.

[18] Suzuki K, Hayashi N, Miyamoto Y, Yamamoto M, Ohkawa K, Ito Y, et al. Expression of vascular permeability factor/vascular endothelial growth factor in human hepatocellular carcinoma. Cancer Res 1996; 56:3004–3009.

[19] Yamaguchi R, Yano H, Nakashima Y, Ogasawara S, Higaki K, Akiba J, et al. Expression and localization of vascular endothelial growth factor receptors in human hepatocellular carcinoma and non-HCC tissues. Oncol Rep 2000;7:725–729.

[20] Yamaguchi R, Yano H, Iemura A, Ogasawara S, Haramaki M, Kojiro M. Expression of vascular endothelial growth factor in human hepatocellular carcinoma. Hepatology 1998;28:68–77.

[21] Yoshiji H, Kuriyama S, Yoshii J, Yamazaki M, Kikukawa M, Tsujinoue H, et al. Vascular endothelial growth factor tightly regulates in vivo development of murine hepatocellular carcinoma cells. Hepatology 1998;28:1489–1496.

[22] Yoshiji H, Kuriyama S, Hicklin DJ, Huber J, Yoshii J, Miyamoto Y, et al. KDR/Flk-1 is a major regulator of vascular endothelial growth

factor-induced tumor development and angiogenesis in murine hepatocellular carcinoma cells. Hepatology 1999;30:1179–1186.
[23] Gossen M, Bujard H. Tight control of gene expression in mammalian cells by tetracycline-responsive promoters. Proc Natl Acad Sci USA 1992;89:5547–5551.
[24] Yoshiji H, Harris SR, Thorgeirsson UP. Vascular endothelial growth factor is essential for initial but not continued in vivo growth of human breast carcinoma cells. Cancer Res 1997;57:3924–3928.
[25] Yoshiji H, Yoshii J, Ikenaka Y, Noguchi R, Yanase K, Tsujinoue H, et al. Suppression of the renin-angiotensin system attenuates vascular endothelial growth factor-mediated tumor development and angiogenesis in murine hepatocellular carcinoma cells. Int J Oncol 2002;20: 1227–1231.
[26] Yoshiji H, Kuriyama S, Yoshii J, Ikenaka Y, Noguchi R, Hicklin DJ, et al. Synergistic effect of basic fibroblast growth factor and vascular endothelial growth factor in murine hepatocellular carcinoma. Hepatology 2002;35:834–842.
[27] Manzotti C, Audisio RA, Pratesi G. Importance of orthotopic implantation for human tumors as model systems: relevance to metastasis and invasion. Clin Exp Metastasis 1993;11:5–14.
[28] Kuriyama S, Yamazaki M, Mitoro A, Tsujimoto T, Kikukawa M, Tsujinoue H, et al. Hepatocellular carcinoma in an orthotopic mouse model metastasizes intrahepatically in cirrhotic but not in normal liver. Int J Cancer 1999;80:471–476.
[29] Lyden D, Hattori K, Dias S, Costa C, Blaikie P, Butros L, et al. Impaired recruitment of bone-marrow-derived endothelial and hematopoietic precursor cells blocks tumor angiogenesis and growth. Nat Med 2001;7:1194–1201.
[30] Hattori K, Heissig B, Wu Y, Dias S, Tejada R, Ferris B, et al. Placental growth factor reconstitutes hematopoiesis by recruiting VEGFR1(+) stem cells from bone-marrow microenvironment. Nat Med 2002;8: 841–849.
[31] Yoshiji H, Kuriyama S, Hicklin DJ, Huber J, Yoshii J, Ikenaka Y, et al. The vascular endothelial growth factor receptor KDR/Flk-1 is a major regulator of malignant ascites formation in the mouse hepatocellular carcinoma model. Hepatology 2001;33:841–847.
[32] Prewett M, Huber J, Li Y, Santiago A, O'Connor W, King K, et al. Antivascular endothelial growth factor receptor (fetal liver kinase 1) monoclonal antibody inhibits tumor angiogenesis and growth of several mouse and human tumors. Cancer Res 1999;59:5209–5218.
[33] Yoshiji H, Kuriyama S, Kawata M, Yoshii J, Ikenaka Y, Noguchi R, et al. The angiotensin-i-converting enzyme inhibitor perindopril suppresses tumor growth and angiogenesis: possible role of the vascular endothelial growth factor. Clin Cancer Res 2001;7: 1073–1078.
[34] Yoshiji H, Harris SR, Raso E, Gomez DE, Lindsay CK, Shibuya M, et al. Mammary carcinoma cells over-expressing tissue inhibitor of metalloproteinases-1 show enhanced vascular endothelial growth factor expression. Int J Cancer 1998;75:81–87.
[35] Yoshii J, Yoshiji H, Kuriyama S, Ikenaka Y, Noguchi R, Okuda H, et al. The copper-chelating agent, trientine, suppresses tumor development and angiogenesis in the murine hepatocellular carcinoma cells. Int J Cancer 2001;94:768–773.
[36] Takahashi T, Shibuya M. The 230 kDa mature form of KDR/Flk-1 (VEGF receptor-2) activates the PLC-gamma pathway and partially induces mitotic signals in NIH3T3 fibroblasts. Oncogene 1997;14: 2079–2089.
[37] O'Reilly MS, Holmgren L, Chen C, Folkman J. Angiostatin induces and sustains dormancy of human primary tumors in mice. Nat Med 1996;2:689–692.
[38] Browder T, Butterfield CE, Kraling BM, Shi B, Marshall B, O'Reilly MS, et al. Antiangiogenic scheduling of chemotherapy improves efficacy against experimental drug-resistant cancer. Cancer Res 2000; 60:1878–1886.
[39] Hlatky L, Hahnfeldt P, Folkman J. Clinical application of antiangiogenic therapy: microvessel density, what it does and doesn't tell us. J Natl Cancer Inst 2002;94:883–893.
[40] Brekken RA, Huang X, King SW, Thorpe PE. Vascular endothelial growth factor as a marker of tumor endothelium. Cancer Res 1998;58: 1952–1959.
[41] Benjamin LE, Keshet E. Conditional switching of vascular endothelial growth factor (VEGF) expression in tumors: induction of endothelial cell shedding and regression of hemangioblastoma-like vessels by VEGF withdrawal. Proc Natl Acad Sci USA 1997;94:8761–8766.

Fulminant hepatic failure caused by malignant melanoma of unknown primary origin

To the Editor: Although malignant melanoma in advanced stages metastasizes widely to many organs, including the liver, liver dysfunction caused by metastatic malignant melanoma is not usually severe. However, malignant melanoma occasionally occurs as an apparent metastasis to lymph nodes or viscera, without a detectable or known primary lesion. We present here a case of fulminant hepatic failure caused by malignant melanoma of unknown primary origin.

A 56-year-old woman was referred to our hospital for the evaluation of generalized malaise of 4-week duration; and anorexia, abdominal distension, and leg edema of 1 week duration. On admission, she was not disoriented, and vital signs were unremarkable. No pigmentation and no superficial nodular lesions were observed anywhere on her body. The liver was palpable 8 cm below the costal margin. Pertinent serum biochemical parameters were as follows: total protein, 5.4 g/dl; albumin, 2.7 g/dl; total bilirubin, 3.4 mg/dl; aspartate aminotransferase (AST), 491 IU/l; alanine aminotransferase (ALT), 204 IU/l; alkaline phosphatase (ALP), 1080 IU/l; and γ-glutamyl transpeptidase (γ-GTP), 198 IU/l. Serum lactate dehydrogenase (LDH) level was extremely high, at 11737 IU/l. Prothrombin activity was 42%. Results of serological studies for hepatitis B and C viruses were negative.

Ultrasonography revealed marked hepatomegaly, mild splenomegaly, and a small amount of ascites. The liver was almost completely occupied by massively infiltrating tumors consisting of low- and high-echoic lesions. Computed tomography (CT) demonstrated that the liver was markedly swollen, and that the massive tumor had disseminated and infiltrated pervasively through almost the entire liver (Fig. 1A). The inferior vena cava was slightly depressed by the tumor, and swelling of mesenteric lymph nodes was observed. Magnetic resonance imaging (MRI) revealed that the right hepatic lobe and the internal segment of the left hepatic lobe were diffusely infiltrated by the tumor, and there were a number of metastatic lesions in the lateral segment of the left hepatic lobe. The hepatic mass showed high intensity on a T1-weighted image (Fig. 1B). There were no tumors in the lung, mediastinum, or neck. The ascites was clear light yellow, and no malignant cells were detected.

On the fifth day of hospitalization, the patients levels of AST, ALT, total bilirubin, and LDH were elevated, to 1006 IU/l, 424 IU/l, 8.0 mg/dl, and 12725 IU/l, respectively. Prothrombin ac-

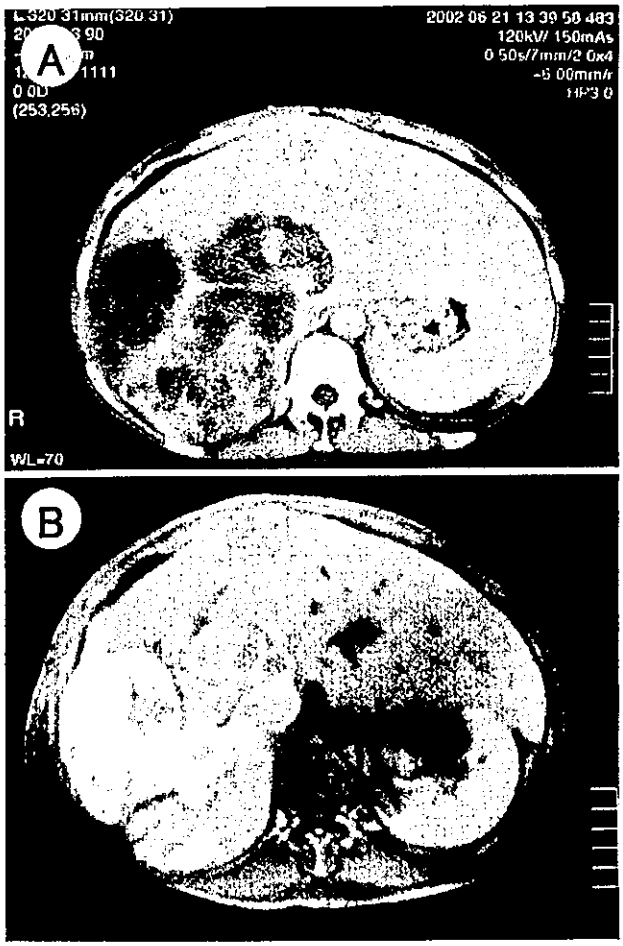

Fig. 1. A Abdominal computed tomography (CT) demonstrated that the liver was markedly swollen, and that a massive tumor had disseminated and infiltrated pervasively through almost the entire liver. B The hepatic mass showed high intensity on a T1-weighted magnetic resonance image

Fig. 2. A Autopsy revealed that the liver was almost completely occupied by a huge black mass, with the weight of the liver being 3850 g. B Histologically, clusters of malignant melanoma cells (*right*) were observed adjacent to hemorrhagic necrosis (*left*). H&E, × 40

tivity was decreased to 29%. On the seventh hospital day, the patient's condition began to deteriorate rapidly due to the progression of hepatic failure and the onset of stage III encephalopathy. She expired within 10 h of the onset of the encephalopathy. Autopsy revealed that the liver was almost completely occupied by a huge black mass, with the weight of the liver being 3850 g (Fig. 2A). There were also black-colored mesenteric lymph nodes. No other remarkable findings were observed in the viscera. Because metastatic malignant melanoma was considered from these autopsy findings, we carefully investigated the whole body, including head, neck, and eyes. However, no primary lesion was detected. Histological findings revealed that clusters of malignant melanoma cells had infiltrated diffusely into the liver parenchyma. The melanoma cells were polygonal, with intracellular melanin pigment (Fig. 2B). Mesenteric lymph nodes also consisted of malignant melanoma cells.

Fulminant hepatic failure is defined as acute liver failure complicated by encephalopathy that occurs within 8 weeks after the onset of symptoms. Although the liver is a common site for the metastatic spread of various malignant diseases, hepatic involvement is usually mild, and fulminant hepatic failure is an unusual presentation of metastatic liver diseases. We examined the previous literature and found only two cases of fulminant hepatic failure secondary to malignant melanoma.[1,2] Harrison et al.[3] reported three patients with metastatic liver disease presenting with a clinical course compatible with fulminant hapatic failure. These three patients had high serum values for aminotransferase and LDH, and all three expired within 1–12 days after hospitalization. McGuire et al.[4] reported four patients with small-cell carcinoma of the lung manifesting as acute hepatic failure. Interestingly, they demonstrated that their was a considerable disparity between serum LDH and aminotransferase levels, and they suggested that the serum LDH level might be the most useful indicator of an underlying neoplastic process. Te et al.[2] reported patient with malignant melanoma with liver metastases that rapidly progressed to fulminant hepatic failure, and death. Striking elevation of values for liver-related parameters was observed. Specifically, the serum level of LDH increased from 3350 IU/l to 31 410 IU/l in 6 days. Therefore, it is suggested that the marked elevation of LDH in patients with metastatic liver diseases is not a simple reflection of acute liver disease, but an ominous sign of impending fulminant hepatic failure. Fulminant hepatic failure carries an extremely high risk of mortality; it appears that measurement of LDH may be useful for identifying patients who are at high risk of developing fulminant hepatic failure, thus allowing the initiation of appropriate treatments.

Misuzu Tanaka, Seishiro Watanabe, Tsutomu Masaki, Kazutaka Kurokohchi, Fumihiko Kinekawa, Hideyuki Inoue, Naohito Uchida, and Shigeki Kuriyama
Third Department of Internal Medicine, Kagawa University School of Medicine, 1750-1 Ikenobe, Miki-cho, Kita-gun, Kagawa 761-0793, Japan

References

1. Bouloux PM, Scott RJ, Goligher JE, Kindell C. Fulminant hepatic failure secondary to diffuse liver infiltration by melanoma. J R Soc Med 1986;79:302–3.
2. Te HS, Schiano TD, Kahaleh M, Lissoos TW, Baker AL, Hart J, et al. Fulminant hepatic failure secondary to malignant melanoma: case report and review of the literature. Am J Gastroenterol 1999;94:262–6.
3. Harrison HB, Middleton HM 3rd, Crosby JH, Dasher MN Jr. Fulminant hepatic failure: an unusual presentation of metastatic liver disease. Gastroenterology 1981;80:820–5.
4. McGuire BM, Cherwitz DL, Rabe KM, Ho SB. Small-cell carcinoma of the lung manifesting as acute hepatic failure. Mayo Clin Proc 1997;72:133–9.

Received: July 7, 2003 / Accepted: November 4, 2003
Reprint requests to: S. Kuriyama
DOI 10.1007/s00535-003-1379-1

Reduced Expression of Cell Cycle Regulator $p18^{INK4C}$ in Human Hepatocellular Carcinoma

Asahiro Morishita,[1] Tsutomu Masaki,[1] Hitoshi Yoshiji,[3] Seiji Nakai,[1] Tomohiro Ogi,[1] Yoshiaki Miyauchi,[1] Shuhei Yoshida,[1] Toshiharu Funaki,[1] Naohito Uchida,[1] Yuko Kita,[1] Fumi Funakoshi,[1] Hisashi Usuki,[2] Setsuo Okada,[2] Kunihiko Izuishi,[2] Seishiro Watanabe,[1] Kazutaka Kurokohchi,[1] and Shigeki Kuriyama[1]

Cyclins, cyclin-dependent kinases (Cdks), and Cdk inhibitors (CdkIs) are frequently altered in human cancer. $p18^{INK4C}$, a member of the INK4 family of CdkIs, is a potential tumor-suppressor gene product. However, the expression of $p18^{INK4C}$ in hepatocellular carcinoma (HCC) remains unknown. The aim of this study was to examine the expression of $p18^{INK4C}$ in various liver diseases including HCC and to assess its clinical significance in HCC. To that end, we examined the expression of $p18^{INK4C}$ by immunohistochemistry in various liver diseases, including 51 HCCs, and also studied the relationship between $p18^{INK4C}$ expression, the phosphorylation of retinoblastoma protein (pRb), and the activity level of Cdk4 and Cdk6. Immunohistochemical analysis revealed the frequent loss of $p18^{INK4C}$ expression in HCC, especially in poorly differentiated HCC. The loss of $p18^{INK4C}$ expression was shown to be associated with a poor prognosis compared with that associated with $p18^{INK4C}$- positivity. Further, the kinase activity of Cdk4 was found to be higher in $p18^{INK4C}$-negative HCCs than in $p18^{INK4C}$- positive HCCs. However, the level of Cdk6 activity was similar in the 2 groups of HCCs. In $p18^{INK4C}$- positive HCCs, $p18^{INK4C}$ dominantly interacted with Cdk4 rather than with Cdk6. pRb phosphorylated at serine(Ser) 780 was detected more frequently in $p18^{INK4C}$ - negative than in $p18^{INK4C}$ - positive HCCs. In conclusion, the loss of $p18^{INK4C}$ expression may play a role in the differentiation and development of HCC through the up-regulation of Cdk4 activity. (HEPATOLOGY 2004;40:677–686.)

Recently, we have revealed that the aberrant expression of cell cycle-related proteins is one of the major factors contributing to the development of hepatocellular carcinoma (HCC).[1–3] The cell cycle is mainly governed by various cyclin-dependent kinases (Cdks); the activity is regulated positively by cyclins, and negatively by Cdk inhibitors (CdkIs). It is also regulated by phosphorylation and dephosphorylation events.[4–6] In mammalian cells to date, at least 2 distinct families of CdkIs are known. One, the p21 family, consists of $p21^{CIP1/WAF1}$, $p27^{KIP1}$, and $p57^{KIP2}$, which are general inhibitors of G1 to S in the cell cycle. The other known CdkI family, the inhibitor of Cdk4 (INK4) family, consists of $p16^{INK4A}$, $p15^{INK4B}$, $p18^{INK4C}$, and $p19^{INK4D}$, which specifically inhibit cyclin D-related kinase activity by binding to Cdk4 or Cdk6.[4–6]

The CdkI proteins, potent negative regulators for the cell cycle, are potential tumor-suppressor gene products, and their loss might play an important role in the development of human cancers.[4–11] In fact, loss of INK4 family members such as $p15^{INK4B}$, $p16^{INK4A}$, and $p18^{INK4C}$ by gene mutation, deletion, and/or methylation has been observed in a variety of human cancers.[6–11] Clinical findings have revealed that the loss of $p16^{INK4A}$ expression is associated with poor prognosis for some types of human cancers.[9–11] These studies have suggested that INK4 family members might play a role in the progression and prognosis of human cancers.

Abbreviations: HCC, hepatocellular carcinoma; Cdk, cyclin-dependent kinase; CdkI, cyclin-dependent kinase inhibitor, INK4, inhibitor of Cdk4; NL, normal liver; CH, chronic hepatitis; HBsAg, hepatitis B surface antigen; HCV, hepatitis C virus; HRP, horseradish peroxidase; IgG, immunoglobulin G; pRb; retinoblastoma protein; LI, labeling index; SDS-PAGE, sodium dodecyl sulfate-polyacrylamide gel electrophoresis; GST, glutathione S-transferase; HBV, hepatitis B virus; TNM, tumor regional lymph nodes, distant metastasis.

From the [1]Third Department of Internal Medicine and [2]First Department of Surgery, Kagawa Medical University, Kagawa, Japan, and [3]Third Department of Internal Medicine, Nara Medical University, Nara, Japan.

Received June 16, 2003; accepted May 19, 2004.

Supported, in part, by Grants-in-Aid for Scientific Research (B-14370185 and C-15590654) from the Ministry of Education, Culture, Sports, Science, and Technology of Japan.

Address reprint requests to: Shigeki Kuriyama, M.D., Ph.D., Third Department of Internal Medicine, Kagawa Medical University, 1750-1 Ikenobe, Miki-cho, Kita-gun, Kagawa 761-0793, Japan. E-mail: skuriyam@kms.ac.jp; fax: 81-87-891-2158.

Published online in Wiley InterScience (www.interscience.wiley.com).

DOI 10.1002/hep.20337

Table 1. Relationship Between p18^{INK4C} Immunoreactivity and Clinicopathological Features of HCC

	Patient No. (L.I. [%])	p18^{INK4C} Staining Status			P Value
		Positive (L.I. [%])	Negative (L.I. [%])	Negative Rate (%)	
Sex					
Male	37 (8.5 ± 7.5)	19 (14.6 ± 5.3)	18 (2.3 ± 2.2)	48.6	
Female	14 (7.8 ± 6.7)	8 (12.6 ± 4.4)	6 (1.3 ± 1.2)	42.9	.762
Age (y)					
<65	27 (7.5 ± 6.7)	15 (11.2 ± 3.7)	12 (2.9 ± 1.3)	44.4	
≥65	24 (6.7 ± 5.2)	12 (10.9 ± 3.7)	12 (2.5 ± 1.7)	50.0	.577
Viral Infection					
HCV-positive	45 (8.7 ± 7.2)	26 (13.8 ± 5.0)	19 (1.7 ± 1.6)	42.2	
HBs Ag-positive	6 (6.2 ± 6.1)	1 (21.0 ± 0)	5 (3.2 ± 3.1)	83.3	.195
*Histological grade					
WD/MD	45 (9.5 ± 7.0)	27 (14.0 ± 5.1)	18 (2.7 ± 2.1)	41.3	
PD	6 (0 ± 0)	0 (0 ± 0)	6 (0 ± 0)	100	.024
†TNM stage					
I/II	21 (11.9 ± 7.4)	16 (14.8 ± 5.8)	5 (2.6 ± 2.1)	23.8	
III/IV	30 (5.9 ± 6.1)	11 (12.9 ± 3.8)	19 (2.2 ± 1.8)	63.3	.025

Abbreviations: WD, well-differentiated; MD, moderately differentiated; PD, poorly differentiated.
*Histological grading of HCC was determined using the criteria of the International Working Party.[17]
†TNM stage was determined using the classification proposed by the Internal Union Against Cancer and the American Joint Committee on Cancer.[16]

Some studies on the relationship between p18^{INK4C} and HCC, on topics such as gene methylation of p18^{INK4C} in HCC,[12] involvement of p18^{INK4C} in troglitazone-induced cell cycle arrest of human hepatoma cell lines,[13] and the rate of carcinogen-induced liver tumor in p18^{INK4C} mutant mice,[14] have been reported. However, to our knowledge, the expression of p18^{INK4C} has not yet been thoroughly examined in various liver diseases, including HCC. In this study, therefore, we focused on the relationship between p18^{INK4C} expression and clinical significance in various liver diseases including HCC.

We examined the expression of p18^{INK4C} immunohistochemically by using an avidin-biotin complex plus tyramide signal amplification method for signal enhancement in normal liver (NL), chronic hepatitis (CH), cirrhosis, and HCC. We also evaluated the relationships between p18^{INK4C} expression and the levels of Cdk4 and Cdk6 activity in HCC. In addition, we examined whether the expression of p18^{INK4C} was an important predictor of outcome in patients with HCC. In this article, we report that loss of p18^{INK4C} expression is involved in hepatocarcinogenesis.

Patients and Methods

Patients. Liver biopsy specimens were obtained from 30 patients with CH (22 males and 8 females; mean age, 48.4 ± 15.5 years; range, 21-80 years). Twenty-seven patients with CH were positive for hepatititis C virus (HCV) RNA, and 3 patients with CH were positive for the hepatitis B surface antigen (HBsAg). Of these 30 patients, 8 were in F1, 7 in F2, 6 in F3, and 9 in F4 according to Desmet's classification.[15] Seven NL tissues were obtained from corresponding surgical cases of liver metastasis of colon cancer (5 males and 2 females; mean age, 58.1 ± 4.9 years; range, 52-67 years). These patients were negative for HCV RNA and HBsAg. Tissue samples of HCC were obtained from 51 patients with HCC during surgery (37 males and 14 females; mean age, 62.9 ± 7.2 years; range, 44-75 years). Forty-five patients with HCC were positive for HCV RNA, and 6 patients with HCC HBsAg. The clinical–pathological data for the patients with HCC is shown in Table 1. Of these 51 patients, 8 were in stage I, 13 in stage II, 11 in stage III, and 19 in stage IV according to the criteria of the International Union against Cancer and the American Joint Committee on Cancer.[16] Histological grade of HCC was determined according to the criteria of the International Working Party.[17] The numbers of patients with well-, moderately, and poorly differentiated HCCs were 16, 29, and 6, respectively (Table 1). Tissues were frozen immediately at −70°C. Informed consent was obtained from each patient prior to participation, and the experimental protocol was approved beforehand by the Human Subjects Committee of Kagawa Medical University.

Chemicals and Antibodies. Chemicals were obtained from Sigma Chemical Co. (Tokyo, Japan) or Wako Pure Chemical Co. (Tokyo, Japan). All primary antibodies were purchased from Santa Cruz Biotechnology (Tokyo, Japan). Secondary antibodies were from Amersham Life Science (Tokyo, Japan). Optimal dilutions of antibodies

used for Western blot were as follows: polyclonal antibody H303 (anti-Cdk4), 1:200; polyclonal antibody C-21 (anti-Cdk6), 1:200; polyclonal antibody serine (Ser) 780 (antiphosphoserine Rb), 1:1000; monoclonal antibody TU-02 (α-tubulin), 1:1000; horseradish peroxidase (HRP)-conjugated anti-rabbit immunoglobulin G (IgG), 1:2000; and HRP-conjugated anti-mouse IgG, 1:2000. The phosphorylated Rb polyclonal antibody (Ser 780) reacts only with phosphorylated retinoblastoma protein (pRb) at Ser 780, which is specifically phosphorylated by cyclin D1/Cdk4, and detects a 105 kd protein corresponding to human pRb that includes amino acids 774 to 786.[18]

Immunohistochemical Examination. We prepared 2 μm-thick sections from formalin-fixed, paraffin-embedded tissue blocks. Sections were stained by an avidin-biotin-peroxidase complex method (Funakoshi Chemical, Tokyo, Japan). The detection of $p18^{INK4C}$ was performed by immunohistochemical study using polyclonal antibody M-20 (anti-$p18^{INK4C}$), as described in our previous article.[3] All sections were examined independently by two observers (T.M., S.W.), who were blinded to the clinical information for each case. For each sample, the percentage of nuclei-immunostained cells was estimated per 1,000 cancer cells. In each case, the nuclei staining evaluation for $p18^{INK4C}$ was classified as negative or positive. The decisions made by the two pathologists were fairly consistent. Furthermore, samples that resulted in disagreement on the immunostaining data between two observers (T.M., S.W.) were discussed with a third observer (A.M.), using a multiheaded microscope until agreement between at least two observers was achieved. The mean labeling index (LI) of $p18^{INK4C}$ was 8.4 ± 7.2 in 51 patients with HCC; therefore, for assessment of the expression of $p18^{INK4C}$, we categorized HCCs into 2 groups on the basis of the percentage of HCC cells positive for $p18^{INK4C}$ immunoreactivity: $p18^{INK4C}$ expression negative (<8.4%), and $p18^{INK4C}$ expression positive (≥8.4%). Necrotic areas and edges of the tissue sections were not included in the counting in order to avoid possible immunohistochemical false-positive results.

Tissue Lysates. The tissue lysate was prepared as described in our previous reports.[1, 2] Protein concentration was measured by a dye-binding protein assay using the Bradford method.[19]

Gel Electrophoresis and Western Blot. Sodium dodecyl sulfate-polyacrylamide gel electrophoresis (SDS-PAGE) was performed according to the method of Laemmli,[20] and Western blot was performed as described by Towbin et al.,[21] using primary antibodies and HRP-conjugated secondary antibodies. Immunoreactive proteins were visualized with an enhanced chemiluminescence detection system (Amersham) on X-ray film.

Kinase Assay of Cdk4 and Cdk6. The kinase activities of Cdk4 and Cdk6 were examined by autoradiography, as described in our previous reports.[1, 2]

Analysis of $p18^{INK4C}$-Bound Cdk4 and Cdk6 in HCC. Immunoprecipitation using $p18^{INK4C}$ was performed as described in our previous report.[1, 2] Immunoprecipitates were then applied to 12.5% SDS-PAGE, and $p18^{INK4C}$-bound Cdk4 and Cdk6 were detected by Western blot analysis using antibody for Cdk4 and Cdk 6, respectively.

Densitometric Analysis. Density of the phosphorylated band of Rb fusion protein obtained by autoradiography was quantitated by densitometric scanning.

Statistical Analysis. We performed statistical analysis of the relationship between $p18^{INK4C}$ expression and clinical–pathological parameters by means of the Fisher *t* test, as appropriate. The survival curve was plotted using the Kaplan-Meier method, and differences were analyzed statistically by log-rank test. The relationship between $p18^{INK4C}$ expression and the activity of Cdk4 or Cdk6 was also determined by Scheffe test. In addition, to identify independent predictors in patients with HCC, multivariate analysis using the Cox proportional hazards model was performed.

Results

$p18^{INK4C}$ Expression in NL, CH, and Liver Cirrhosis. Representative immunostaining of $p18^{INK4C}$ in NL (Fig. 1A), CH (Figs. 1B and C), and liver cirrhosis (Fig. 1D) are shown. The stages of fibrosis in Figs. 1B, C, and D were F2, F3, and F4, respectively. The $p18^{INK4C}$ in NL and CH (Figs. 1B and C) was localized in hepatocellular nuclei and/or nonparenchymal cells such as infiltrating lymphocytes (Fig. 1B, arrowhead), fibroblasts (Fig. 1C, arrowhead), and endothelial cells. The expression of $p18^{INK4C}$ was detected in all patients (n = 30) with CH or cirrhosis, regardless of fibrosis staging. As shown in Fig. 1D, the expression of $p18^{INK4C}$ in liver cirrhosis was detected not only in the hepatocellular cytoplasm, but also in the hepatocellular nucleus in all 9 cases. The expression of $p18^{INK4C}$ was detected in the hepatocellular nucleus in all NLs examined in this study.

$p18^{INK4C}$ in Malignant Liver Tissues. As shown in Table 1, $p18^{INK4C}$-negative HCCs were observed in 24 of 51 HCCs (47%; LI, 2.3 ± 2.2%) examined, and $p18^{INK4C}$-positive HCCs were detected in the remaining 27 cases (53%; LI, 14.0 ± 5.1%). In well-differentiated HCCs, 10 of 15 tumor samples were positively stained in the nucleus of cancer cells for $p18^{INK4C}$ (67%; LI, 15.2 ±

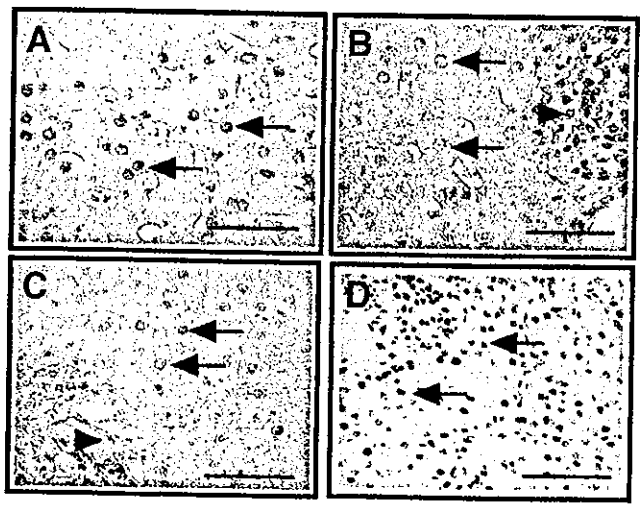

Fig. 1. Immunohistochemistry of $p18^{INK4C}$ in liver tissues of (A) normal liver, (B and C) chronic hepatitis, and (D) liver cirrhosis. Fibrosis stages in panels B, C, and D were grades F2, F3, and F4, respectively, according to Desmet's classification. Staining for $p18^{INK4C}$ in normal liver and chronic hepatitis was seen (A-C) in the hepatocellular nucleus (**arrows**)), (B) in lymphocytes (**arrowhead**), and (C) in fibroblasts (**arrowhead**). Expression of $p18^{INK4C}$ in liver cirrhosis was positive not only for $p18^{INK4C}$ staining in the hepatocellular cytoplasm but also for $p18^{INK4C}$ staining in (D) the hepatocellular nucleus (**arrows**). **Scale bars**, 50 μm. (Original magnification [A-D], ×200.)

6.7%; Figs. 2A-C), and the remaining cases were negative for staining (33%; LI, 3.8 ± 1.6%). In moderately differentiated HCCs, $p18^{INK4C}$-positive HCCs were detected in 17 of 30 cases (57%; LI, 13.4 ± 3.8%) and not in the remaining cases (43%; LI, 2.7 ± 2.2%; Figs. 2D-F). In poorly differentiated HCCs, $p18^{INK4C}$-positive HCCs were not detected in any of the cases examined in this study (Figs. 2G-I: LI, 0.0 ± 0.0 %).

Correlations between $p18^{INK4C}$ expression and clinical–pathological factors as determined by univariate analysis are summarized in Table 1. The ratio of $p18^{INK4C}$-positive HCCs in poorly differentiated tissues (LI, 0.0 ± 0.0%) was significantly lower than that in well-differentiated and moderately differentiated tissues (LI, 14.0 ± 5.1%; Table 1, $P = .024$). In addition, the ratio of $p18^{INK4C}$-negative HCCs in tumor stages III and IV (63.3%) was significantly higher than that in tumor stages I and II (23.8 %; $P = .025$). However, no significant relationship was seen between $p18^{INK4C}$ expression and gender, age, or viral markers.

Prognostic Significance of $p18^{INK4C}$. Survival analysis of HCC was performed by the Kaplan-Meier method. The tumors were divided into $p18^{INK4C}$-positive and $p18^{INK4C}$-negative groups. Patients with $p18^{INK4C}$-negative HCC had a significantly worse prognosis than those with $p18^{INK4C}$-positive HCC ($P = .0007$; Fig. 3). Multivariate analysis using the Cox proportional hazards model was performed. Among age, sex, histological grade, tumor stage, and hepatitis viral infection, only tumor stage and $p18^{INK4C}$ expression were shown to be independent prognostic factors for overall survival of patients with HCC (Table 2).

Activities and Amounts of Cdk4 and Cdk6 in HCC. $p18^{INK4C}$ has been shown to inhibit cyclin D1- related

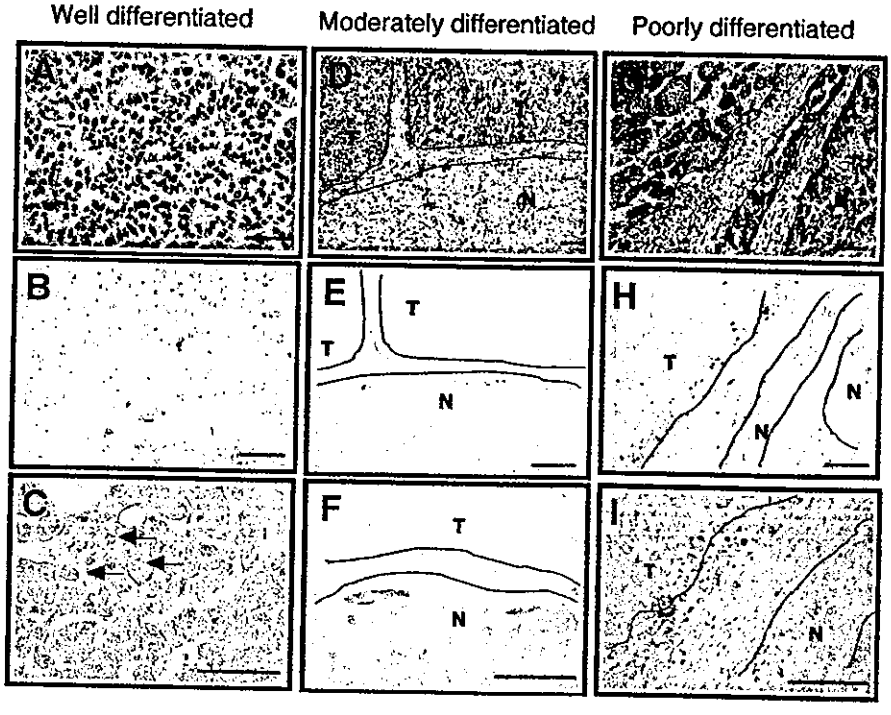

Fig. 2. Immunohistochemistry of $p18^{INK4C}$ in (B and C) well-, (E and F) moderately, and (H and I) poorly differentiated HCCs. A, D and G show hematoxylin-eosin staining of the section adjacent to B, E, and H, respectively. C, F, and I represent higher magnifications of the sections of B, E, and H, respectively. T and N indicate HCC and nontumorous tissues with cirrhosis, respectively. The expression of $p18^{INK4C}$ in most well-differentiated HCCs was localized in the nuclei of cancer cells (**arrows**). Conversely, its expression in most moderately and poorly differentiated HCCs was not detected. The scar indicates the boundary between N and T tissues. **Scale bars**, 50 μm.(Original magnification: A, B, E, and H, ×100; D and G, ×50; and C, F, and I, ×200.)

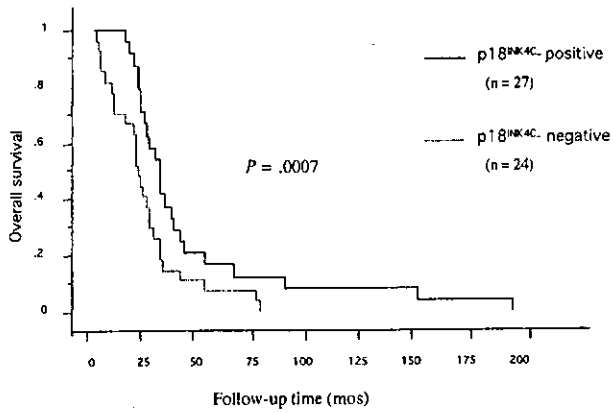

Fig. 3. Kaplan-Meier curves of overall survival according to $p18^{INK4C}$ expression (positive staining vs. negative staining) in 51 patients with HCC. Time to death was significantly shorter in patients with $p18^{INK4C}$-negative HCCs than in those with $p18^{INK4C}$-positive HCCs ($P < .0007$).

kinase activity specifically by binding Cdk4 or Cdk6. Therefore, to examine the role of $p18^{INK4C}$ in the control of cell proliferation via inhibition of Cdk4 or Cdk6 activities in the G1 to S phase, we studied the activity of Cdk4 and Cdk6 in 38 HCC cases, including 12 well-differentiated, 20 moderately differentiated, and 6 poorly differentiated tumors. Clinical–pathological data for the 38 patients with HCC are shown in Table 3. $p18^{INK4C}$-negative HCCs were 21 (55 %) out of 38, with the remaining 17 (45 %) $p18^{INK4C}$-positive. Glutathione S-transferase (GST)-Rb fusion protein was used as a substrate to measure the Cdk4 and Cdk6 activity. As shown in Fig. 4A, staining of the GST-Rb fusion protein after separation by SDS-PAGE showed a single band with a molecular size of 46 kd. The activities of Cdk4 and Cdk6 were measured by an *in vitro* kinase assay using the GST-Rb fusion protein as a substrate (Figs. 4B and C). A single band of phosphorylated GST-Rb fusion protein resulting from the level of Cdk4 and Cdk6 activity was detected in all HCCs studied. Additionally, phosphorylated GST-Rb fusion protein was not observed in the immunoprecipitate product when nonimmune rabbit IgG was used as a control (data not shown). Extremely enhanced Cdk4 activity was detected in a subset of $p18^{INK4C}$-negative HCCs (Fig 4B, patients 6 and 7). In moderately differentiated HCCs, the number of $p18^{INK4C}$-negative HCCs and $p18^{INK4C}$-positive HCCs was 10 and 10, respectively. In moderately differentiated HCCs, Cdk4 activity of $p18^{INK4C}$-negative and $p18^{INK4C}$-positive HCCs were 9.8 ± 6.4 and 4.1 ± 1.4 times higher, respectively, than those of control NLs (Fig. 4D). Cdk4 activity in $p18^{INK4C}$-negative moderately differentiated HCCs was significantly higher than that in $p18^{INK4C}$-positive HCCs ($^*P < .02$). Conversely, Cdk6 activity of moderately differentiated HCCs did not change regardless of expression of $p18^{INK4C}$ (Fig. 4 D). In well-differentiated HCCs, the number of $p18^{INK4C}$-negative HCCs and positive HCCs was 7 and 5, respectively. Although Cdk 6 activity remained at a similar level regardless of $p18^{INK4C}$ expression in well-differentiated HCCs, Cdk4 activity in $p18^{INK4C}$-negative HCCs was significantly higher than that in $p18^{INK4C}$-positive HCCs ($^*P < .05$; Fig. 4E). The kinase activity levels of Cdk4 and Cdk6 in poorly differentiated HCCs were 16.6 ± 3.8 and 2.8 ± 1.3, respectively (data not shown). We then ana-

Table 2. Multivariate Cox Model Analysis of Overall Survival of Patients With HCC

	Hazards Ratio	Overall Survival 95% CI	*P* Value
Age (<65/≥65)	0.870	0.407-1.860	.719
Sex (male/female)	0.821	0.354-1.902	.645
Histology (PD/WD, MD)	1.380	0.443-4.306	.579
Tumor stage (III-IV/I-II)	2.595	1.077-6.257	.034
Infection (HCV/HBV)	0.772	0.300-1.982	.590
$p18^{INK4C}$ (negative/positive)	2.725	1.155-6.427	.022

Abbreviations: PD, poorly differentiated; WD, well-differentiated; MD, moderately differentiated.

Table 3. Characteristics of HCC Patients Examined for Cdk4 and Cdk6 Activity

Sex	
Male	25
Female	13
Age (y)	
Mean ± SD	63.8 ± 6.5
Range	44-75
Viral infection	
HCV-positive	33
HBsAg-positive	5
*Histological background	
F3	6
F4	32
†Histological differentiation	
WD	12
MD	20
PD	6
$p18^{INK4C}$ expression	
Positive	17
Negative	21
‡TNM stage	
I	13
II	10
III	8
IV	7

Abbreviations: WD, well-differentiated; MD, moderately differentiated; PD, poorly differentiated; TNM, tumor regional lymph nodes, distant metastasis.

*The fibrosis stage of the tissue surrounding HCC was assessed according to Desmet's classification.

†Histological grading of HCC was determined using criteria of the International Working Party.[17]

‡TNM stage was determined using the classification proposed by the International Union Against Cancer and the American Joint Committee on Cancer.[16]

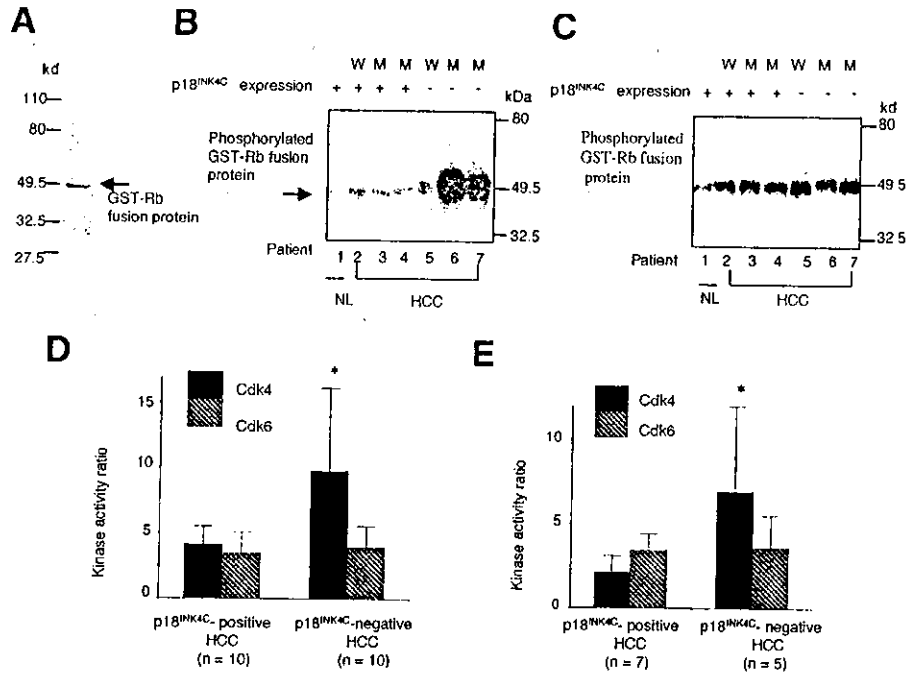

Fig. 4. Activity of Cdk4 and Cdk6 in HCC. (A) SDS-PAGE profile of a glutathione-S transferase (GST)-Rb fusion protein. Staining showed a single band of 46 kd (**arrow**). (B) Cdk4 and (C) Cdk6 kinase assays in NL and HCC. Lysates containing 500 μg of total cellular protein were prepared as described in Materials and Methods. The protein was precipitated with excess Cdk4 or Cdk6 antibodies, incubated for 10 minutes at 30°C with [γ-^{32}P] ATP and GST-Rb fusion protein, then resolved on 12.5% SDS-polyacrylamide gel. (B) The **arrow** indicates the band corresponding to the phosphorylation of GST-Rb fusion protein. (B and C) The immunostaining pattern of $p18^{INK4C}$ in NL and HCC is indicated as positive (+) or negative (−). W, well-differentiated HCC; M, moderately differentiated HCC. Note that extremely enhanced Cdk4 activity was seen in a subset of $p18^{INK4C}$-negative HCCs, but Cdk6 activity level was similar regardless of $p18^{INK4C}$ expression. The relative levels of Cdk4 and Cdk6 activity in (D) moderately differentiated and (E) well-differentiated HCCs in $p18^{INK4C}$-positive and -negative HCCs. Cdk4 activity of $p18^{INK4C}$-negative HCCs was significantly higher than that of $p18^{INK4C}$-positive HCCs when measured by the phosphorylation of GST-Rb fusion protein, whereas Cdk6 activity was not significantly different between $p18^{INK4C}$-positive and $p18^{INK4C}$-negative HCCs, regardless of differentiation. $^*P < .05$ compared with HCC $p18^{INK4C}$-positive HCCs.

lyzed whether one of the pRb phosphorylation sites, Ser 780, was phosphorylated. The phosphorylated pRb band was detected in $p18^{INK4C}$-negative HCCs (Fig. 5A). A band corresponding to the pRb phosphorylated at Ser 780 was detected in 18 (86%) of 21 $p18^{INK4C}$-negative HCCs, and in 2 (12%) of 17 $p18^{INK4C}$-positive HCCs. The expression levels of Cdk4 and Cdk6 were measured by Western blot. In HCC, Cdk4 (Fig. 5B) and Cdk6 (Fig. 5C) immunoreactive bands were detected at molecular weights of 34 kd and 38 kd, respectively. As an internal control, the amount of α-tubulin was almost the same in each lane (Fig. 5D). Protein levels of Cdk4 and Cdk6 were almost the same in $p18^{INK4C}$-negative and $p18^{INK4C}$-positive HCCs in not only moderately differentiated HCCs (Fig. 5E) but also in well-differentiated HCCs (Fig. 5F).

Detection of $p18^{INK4C}$-Bound Cdk4 and Cdk6 in HCC. Immunoprecipitates with an anti-$p18^{INK4C}$ antibody obtained from 17 HCCs were immunoblotted with an anti-Cdk4 or anti-Cdk6 antibody. Clinical–pathological data for these 17 patients with HCC are shown in Table 4. Patients 2, 3, and 4 in Fig. 5G correspond to F.O., N.S., and Y.K., respectively. As shown in Fig. 5G and Table 4, $p18^{INK4C}$-bound Cdk4 was detected in 16 patients (94%), including HCCs from patients 2 (F.O.), 3 (N.S.), and 4 (Y. K.), and was not detected in one case (R.K.). $p18^{INK4C}$-bound Cdk6 was detected in 2 cases (12%), including HCCs from patient 2 (F.O.), but not in any other cases (Fig. 5G, Table 4). $p18^{INK4C}$-bound Cdk4 was also detected in 2 cases (F.O. and F.E.) with interaction between Cdk6 and $p18^{INK4C}$ (Table 4).

Discussion

CdkIs regulate the progression of the cell cycle by modulating the activity of Cdks.[9] Inactivation of CdkIs has been associated with neoplastic transformation in a large number of human epithelial tissues.[5,6] Moreover, recent studies have extensively demonstrated that the inactivation of $p16^{INK4A}$ in the members of the INK4 family leads to the development and aggression of a number of human malignancies including HCC.[7–11] These previous studies

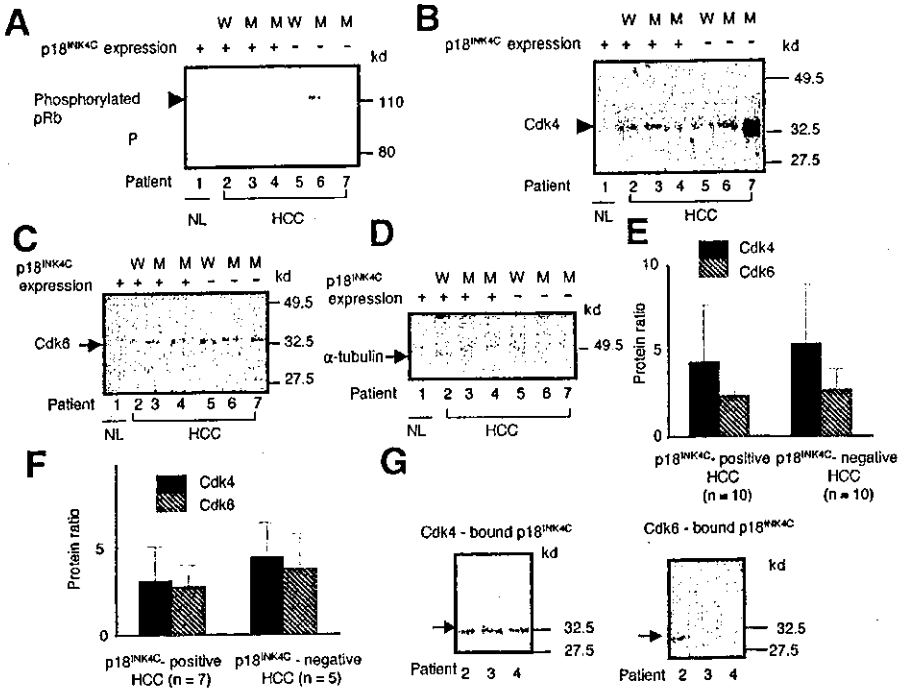

Fig. 5. Amounts of Cdk4 and Cdk6 in HCC. (A) Representative Western blot of retinoblastoma protein (pRb) using an antibody against phosphorylated pRb (Ser 780) in normal liver (NL) and HCC. The phosphorylation of pRb was detected in HCCs negative for $p18^{INK4C}$ expression, but not in those positive for $p18^{INK4C}$ expression. Western blot of (B) Cdk4, (C) Cdk6, and (D) α-tubulin in NL and HCC. The relative amount of Cdk4 and Cdk6 in (E) moderately differentiated HCC and (F) well-differentiated HCC in $p18^{INK4C}$-positive and - negative HCCs. Note that the amounts of Cdk4 and Cdk6 in $p18^{INK4C}$-positive and $p18^{INK4C}$-negative HCCs did not significantly differ. (G) Amounts of Cdk4-bound $p18^{INK4C}$ and Cdk6-bound $p18^{INK4C}$ in $p18^{INK4C}$- positive HCCs. Note that the complex of Cdk6 and $p18^{INK4C}$ was not seen in the liver tissues of patients 3 and 4 with $p18^{INK4C}$-positive HCC but was detected in the liver tissue of patient 2 (**arrow**). Cdk4-bound $p18^{INK4C}$ was detected in these same patients (2, 3, and 4; **arrow**). W, well-differentiated HCC; M, moderately differentiated HCC.

suggested that the other INK4 family might also play a role in the progression and prognosis of human cancers. Recently, inactivation of $p18^{INK4C}$ has been reported in various human cancers.[22–25] To date, very little data is available on the relationship between $p18^{INK4C}$ and HCC,[12] though previous reports have investigated gene methylation of $p18^{INK4C}$ in HCC, involvement of $p18^{INK4C}$ in troglitazone-induced cell cycle arrest of hepatoma cell lines,[13] and the rate of carcinogen-induced liver tumor in $p18^{INK4C}$ mutant mice.[14] The expression of $p18^{INK4C}$ protein in HCC is not yet known. In the present study, therefore, we evaluated the expression of $p18^{INK4C}$ in various liver diseases including HCC. To our knowledge, this study is the first to assess the involvement of $p18^{INK4C}$ protein in hepatocarcinogenesis.

The major finding in this study was that the loss of $p18^{INK4C}$ does not occur in most NL, CH, and cirrhosis, but does occur in a subset of HCCs, especially in poorly differentiated HCCs, suggesting that loss of $p18^{INK4C}$ is involved in hepatocarcinogenesis. The levels of Cdk4 activity in $p18^{INK4C}$-negative HCCs were significantly higher than those in $p18^{INK4C}$- positive HCCs, underscoring the functional importance of $p18^{INK4C}$ as an inhibitor of Cdk4 in HCC. It has been shown that the loss of $p18^{INK4C}$ expression in HCC is a poor prognostic marker.

Evidence suggests that $p18^{INK4C}$ functions as a tumor suppressor. Some studies using gene knockout mice indicated that the loss of $p18^{INK4C}$ displays a variety of aberrant phenotypes including lymphoproliferative disorders, organomegaly, and pituitary gland hyperplasia. Double knockout mice for $p18^{INK4C}$ and other members of the CdkI family display more varied and pronounced phenotypes,[26–28] indicating that $p18^{INK4C}$ is important for the proliferative control of various cell lineages. On the relationship between hepatocarcinogenesis and p 18^{INK4C}, Bai et al.[14] reported that $p18^{INK4C}$-null and -heterozygous mice with chemical carcinogen results in tumor development at an accelerated rate, suggesting that loss and decrease of $p18^{INK4C}$ leads to malignant transformation. In addition, the $p18^{INK4C}$ gene has been mapped to chromosome 1q32, where chromosomal translocation or loss has been found in various human cancers including HCC.[29–33] Such events might explain the loss in $p18^{INK4C}$ protein expression found in a subset of HCC in this study. A marked decrease in $p18^{INK4C}$ protein level